

# A review of wastewater treatment technologies for the degradation of pharmaceutically active compounds: carbamazepine as a case study

Sara Feijoo<sup>1</sup>, Mohammadreza Kamali<sup>1</sup>, and Raf Dewil<sup>1,2,\*</sup>

<sup>1</sup> KU Leuven, Department of Chemical Engineering, Process and Environmental Technology Lab, Sint-Katelijne-Waver, Belgium

<sup>2</sup> University of Oxford, Department of Engineering Science, Parks Road, Oxford, OX1 3PJ, United Kingdom

\*Corresponding author: Raf Dewil, raf.dewil@kuleuven.be

**Keywords** – Carbamazepine, advanced oxidation processes (AOPs), advanced reduction processes (ARPs), biological treatments, physical treatments, wastewater

## Abstract

The potential toxicological effects of pharmaceutically active compounds (PhACs) in natural water bodies have received considerable critical attention over the past years, encouraging numerous researchers to develop novel technologies to address the limitations of current wastewater treatment methods. Among the wide range of reported PhACs, carbamazepine is a well-known anticonvulsant that has often been used as a target compound in various studies because of its prevalence and resistance against degradation. The aim of this article is to summarize the research progress attained to date regarding the removal of this pharmaceutical as well as to evaluate and compare the performance of biological, physical, chemical and hybrid treatments. The review conducted on the available literature revealed that novel advanced oxidation processes (AOPs) and advanced reduction processes (ARPs) are a comprehensive set of promising techniques with an outstanding effectiveness, as most treatments allow for degradation rate constants in the order of 4 to 12 h<sup>-1</sup>, meaning that 99% carbamazepine removal can be attained in less than 70 min under optimal conditions. In particular, electrochemical and photocatalytic AOPs have consistently reported successful degradation results.

**Abbreviations:** AC: Activated carbon, AOP(s): Advanced oxidation process(es), API: Active pharmaceutical ingredient, ARP(s): Advanced reduction process(es), BDD: Boron-doped diamond, CAS: Conventional activated sludge, CBZ: Carbamazepine, CEC(s): Contaminant(s) of emerging concern, COD: Chemical oxygen demand, DOC: Dissolved organic carbon, DOM: Dissolved organic matter, EO: Electrochemical oxidation, GAC: Granular activated carbon, IW: Industrial wastewater, MBR: Membrane bioreactor, MOF(s): Metal-organic framework(s), MWCO: Molecular weight cut-off, MWWTP: Municipal wastewater treatment plant, NF: Nanofiltration, nZVI: Nano zero valent iron, PAC: Powdered activated carbon, PFAS: Per- and polyfluoroalkyl substances, PhACs: Pharmaceutically active compounds, PMS: Peroxymonosulfate, PPCPs: Pharmaceuticals and personal care products, PS: Persulfate, PNECs: Predicted no-effect-concentrations, RO: Reverse osmosis, TOC: Total organic carbon, US: Ultrasound, UV: Ultraviolet, WW: Wastewater, WWTP: Wastewater treatment plant.

## 1 Introduction

The latest advances in high-accuracy analytical techniques have shed light on the presence of numerous contaminants of emerging concern (CECs) in wastewater streams at concentrations ranging from  $\text{ng L}^{-1}$  to  $\mu\text{g L}^{-1}$  [1–3]. The CEC category refers not only to compounds recently detected in water bodies and whose effects are unknown but also to contaminants that have already been identified and whose persistence is becoming a problematic threat [4–6]. Compounds such as pharmaceutically active compounds (PhACs), pharmaceuticals and personal care products (PPCPs), endocrine disruptors, pesticides, flame retardants, perfluorinated compounds and household chemicals are common CECs found in wastewater that originate from diverse sources (e.g., industries, households, hospitals, landfills, agriculture, irrigation activities, etc.) [1, 7–10]. Numerous studies have highlighted the adverse ecotoxicological and human health effects that CECs may cause both in the short and long term [1, 8, 11–15]. Therefore, considerable research effort has been devoted to the development of novel technologies to solve this ever-rising issue in an effective, cost-efficient and sustainable manner [16–23].

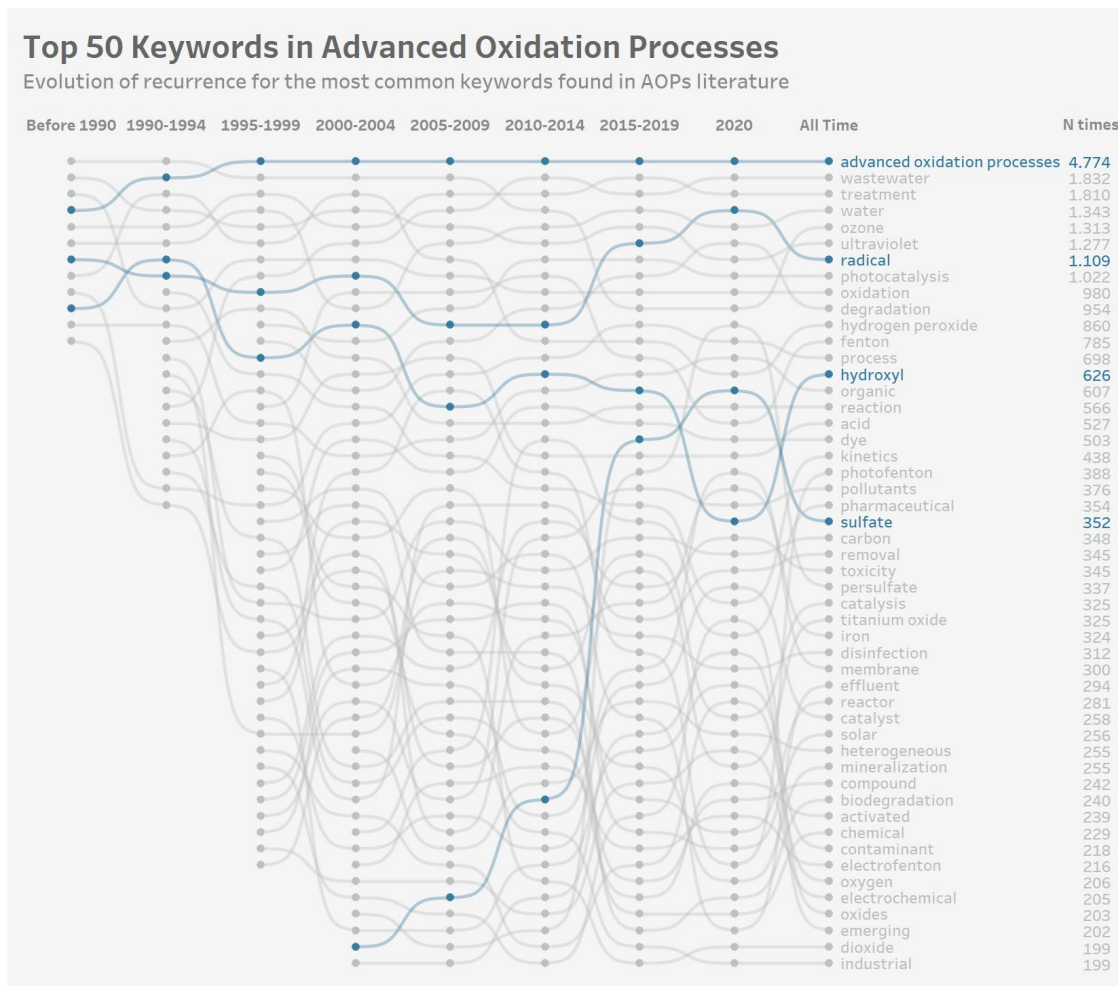
Carbamazepine (CBZ) is a common anticonvulsant primarily used to treat epilepsy and nerve pain by reducing the spread of seizure activity in the brain [24]. It is currently consumed in large quantities worldwide, with an estimated consumption growth from 742 tons in 1995 to 1214 tons in 2015 [25]. After its oral administration, only 72% is absorbed by the human body and metabolized up to a 99% level, while the rest is discharged into the sewage system [26]. Its likelihood for biodegradation, photodegradation and volatilization is negligible, making it a suitable candidate for CEC degradation studies, especially regarding PhACs [26, 27]. In addition, it has been used as a contamination indicator in water and wastewater effluents [28]. In fact, it has been reported as the most frequently detected active pharmaceutical ingredient (API) in river catchments, being found in 62% of the 1,052 sampling sites analyzed along 258 rivers worldwide [29]. The concentration of carbamazepine in water streams has been reported to reach  $23 \text{ ng L}^{-1}$  in drinking water,  $83 \text{ ng L}^{-1}$  in groundwater,  $23 \mu\text{g L}^{-1}$  in surface water,  $200 \mu\text{g kg}^{-1}$  dry weight in sewage sludge and  $259 \mu\text{g L}^{-1}$  in municipal and urban wastewater [11, 30]. These values exceed predicted no-effect concentrations (PNECs) for ecological toxicity (i.e.,  $25 \text{ ng L}^{-1}$ ), becoming a potential threat to aquatic ecosystems [1, 31, 32]. Specifics on the potential toxicological effects of carbamazepine exposure on aquatic species and human health have been reviewed by Hai et al. (2018), where the limited number of studies in the field as well as their diverse results call for additional risk assessments and thorough monitoring [33]. Due to its persistence and increasing presence, carbamazepine has therefore been internationally recognized as a concerning pollutant, included in the NORMAN List of Emerging Substances [30] and classified as an Endocrine Disrupting Chemical by the US Environmental Protection Agency [34].

The issue with the uncontrolled release of PhACs such as carbamazepine lies in the fact that they can eventually terminate into natural systems such as surface water, groundwater and soils, given that conventional (physico)chemical and biological treatments are not designed to achieve their complete elimination [2–4, 10]. Nevertheless, these conventional methods can be used as complementary steps in wastewater treatment since they offer unique advantages, such as being simple and efficient when removing biodegradable compounds as well as economic, environmentally friendly and safe [35, 36]. Among novel treatment methods, advanced oxidation processes (AOPs) have received particular attention over the past years. They are a wide set of technologies that rely on the generation of powerful species, mainly oxidative radicals, to degrade CECs [2, 6, 37, 38]. Similarly, advanced reduction processes (ARPs) operate based on the generation of reductive radicals [39, 40]. In both cases, radicals are species characterized by having an unpaired electron,

95 and thus showing a strong tendency to interact with other compounds to attain an even number of  
96 electrons, either by donating the unpaired one (i.e., acting as a reducing agent) or by accepting  
97 another electron (i.e., acting as an oxidizing agent) [41]. Radical generation methods can be  
98 categorized based on their dependence on energy sources (i.e., electro, sono, thermo or  
99 photochemical processes), an opposed lack of energy requirements (i.e., chemical and catalytic  
100 systems) as well as in case they show a hybrid design. There is a substantial body of literature  
101 regarding AOPs, as they have been shown to be suitable for both the pre- and posttreatment of  
102 contaminated wastewater. The pretreatment operation is preferred for highly toxic water influents  
103 to increase their biodegradability, while posttreatment applications are advised as a polishing step to  
104 increase degradation and mineralization efficiencies [42–44]. In particular, AOPs based on the  
105 generation of hydroxyl radicals ( $\cdot\text{OH}$ ) show the largest contribution, as reflected by previous  
106 scientometric analyses [45, 46]. In parallel, attention has also been dedicated to sulfate radical  
107 ( $\text{SO}_4^{\cdot-}$ )-based AOPs, which despite appearing later, have quickly gained importance in the field (Fig.  
108 1). As further discussed in this review, carbamazepine degradation has accordingly been more  
109 extensively investigated through both types of AOPs than with other treatments.  
110

111 The present article draws on the literature on the removal of carbamazepine from wastewater  
112 streams, including both real and synthetic effluents, to illustrate and compare the performances of  
113 multiple physical, biological and chemical technologies, with a special emphasis on the latter in the  
114 form of AOPs. Further experimental details of the different literature studies under review can be  
115 found in Tables 1 and 2.

116  
117  
118  
119  
120  
121



122  
123  
124  
125  
126  
127  
128  
129

**Figure 1:** Evolution of the Top 50 keywords in the field of AOPs. This ranking is based on the number of times that a specific keyword has appeared in either the title, abstract or author keywords of a certain scientific publication related to the field of AOPs. To this end, the keyword combination [*wastewater OR waste water OR effluent OR water OR aqueous solution*] with [*“advanced oxidation”*] has been applied to all documents indexed in Scopus. Accordingly, 8712 documents were screened, and their corresponding keywords were identified and ranked across time periods of 5 years. The total frequency of each keyword measured until the end of 2020 is shown in the last column. In particular, the keywords *radical*, *hydroxyl* and *sulfate* have been highlighted in the visualization to emphasize their relevance and recurrence.

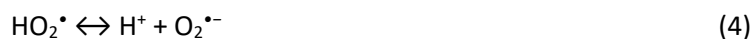
130  
131  
132  
133  
134  
135  
136  
137  
138  
139  
140  
141  
142  
143  
144  
145  
146  
147  
148  
149  
150  
151  
152  
153  
154  
155  
156  
157  
158  
159  
160  
161  
162  
163  
164  
165  
166  
167  
168  
169  
170  
171  
172  
173

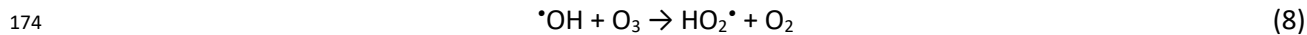
## 2 Advanced oxidation processes

A vast literature exists on the application of advanced oxidation processes (AOPs) for carbamazepine degradation, comprising multiple types of radicals and activation methods. In this review, they have been grouped as (i) chemical and catalytic oxidation, (ii) electrochemical oxidation, and (iii) photo(catalytic)oxidation, depending on the primary activation method for oxidative radicals. For additional information on the underlying mechanisms and operating conditions of each AOP treatment, the reader is referred to the reviews by Cuerda-Correa et al. (2020) [6] and Wang and Zhuan (2020) [47] for  $\cdot\text{OH}$ -based AOPs, and to the reviews by Guerra-Rodríguez et al. (2018) [48] and Giannakis et al. (2021) [49] for  $\text{SO}_4^{\cdot-}$ -based AOPs.

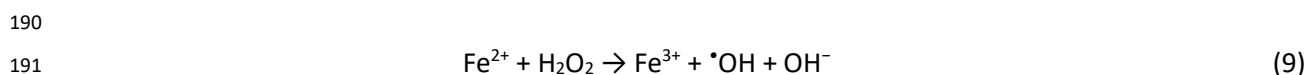
### 2.1 Chemical and catalytic oxidation

Among the chemical-based activation methods, the most relevant AOPs are those degradation systems based on ozonation, Fenton reaction and  $\text{SO}_4^{\cdot-}$  radicals. Ozonation applied to different effluents containing less than  $1 \text{ mg L}^{-1}$  carbamazepine has shown consistent degradation results with efficiencies close to 100% among different studies, with an estimated ozone dosage in the order of  $0.6 \text{ g O}_3/\text{g}$  dissolved organic carbon (DOC) [3, 50, 51]. This is because carbamazepine is characterized by electron-rich moieties that easily react with ozone as well as by the cogeneration of powerful  $\cdot\text{OH}$  and secondary radicals (Eqs. 1-8) [3]. On the downside, ozonation is heavily influenced by the presence of suspended solids, nitrite ions ( $\text{NO}_2^-$ ), and effluent organic matter, which is also likely to present numerous ozone reactive moieties, leading to competition reactions that may hamper carbamazepine removal [3, 52].

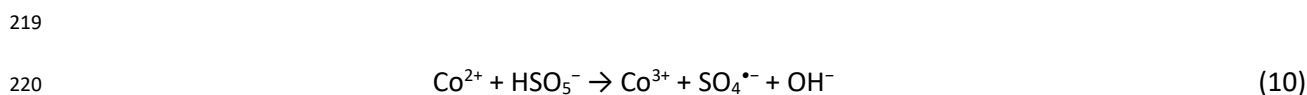




175  
 176 Regarding other  $\cdot\text{OH}$ -based chemical activation methods, the classical Fenton reaction (Eq. 9) has  
 177 been extensively investigated, which is based on the use of hydrogen peroxide ( $\text{H}_2\text{O}_2$ ) and an iron  
 178 catalyst to release  $\cdot\text{OH}$  radicals that yield pollutant degradation [53]. For carbamazepine removal,  
 179 there is quite some variability in the results for Fenton-related treatments, ranging from ca. 7% up to  
 180 100% degradation [54–56]. The key factors affecting the treatment performance are the initial iron  
 181 concentration since higher values yield higher degradation efficiencies, and the complexity of the  
 182 water matrix since chloride ( $\text{Cl}^-$ ), carbonate ( $\text{CO}_3^{2-}$ ) and bicarbonate ( $\text{HCO}_3^-$ ) ions are the main cause  
 183 for  $\cdot\text{OH}$  scavenging, and thus decrease degradation rates [54, 56]. In terms of reported degradation  
 184 rate constants, Matta et al. (2011) attained a value of  $11.34 \text{ h}^{-1}$ , with both  $\text{Fe(II)}$  and  $\text{H}_2\text{O}_2$   
 185 concentrations up to 0.25 mM [54]. In recent years, Fenton processes have also been combined with  
 186  $\text{SO}_4^{\cdot-}$ -based systems, such as in the two-staged nanoscale zero valent iron (nZVI)-activated persulfate  
 187 (PS) and Fenton process investigated by Wu et al. (2020), which yielded 77% carbamazepine  
 188 degradation [57]. The main advantage of this system is the partial substitution of PS by  $\text{H}_2\text{O}_2$ , which  
 189 reduces both operational costs and the release of sulfate ( $\text{SO}_4^{2-}$ ) ions in the effluent [57].



192  
 193 Finally, peroxymonosulfate ( $\text{HSO}_5^-$ , PMS) and persulfate ( $\text{S}_2\text{O}_8^{2-}$ , PS) are two common precursors  
 194 for the generation of  $\text{SO}_4^{\cdot-}$  radicals in conventional  $\text{SO}_4^{\cdot-}$ -based AOPs [58]. Matta et al. (2011) tested  
 195 the activation of PMS for carbamazepine degradation through several cobalt-based catalysts (Eq.  
 196 10). Their results showed that the presence of Cl-substitutes in the catalyst could reduce the  
 197 reaction rate constant by almost 40%, meaning that after 35 min of treatment, the degradation  
 198 percentage could oscillate between 88% and 100% depending on the catalyst used. Additionally, the  
 199 complexity of the water matrix had an inhibitory effect on the degradation, as the final  
 200 carbamazepine removal was 50% after 1 h of treatment in a real wastewater effluent. The maximum  
 201 degradation rate constant obtained in such a system was approximately  $14.87 \text{ h}^{-1}$  [54]. In the case of  
 202  $\text{Fe(II)}$ -activated PS (Eq. 11), opposite results were attained by Rao et al. (2014), as the presence of  $\text{Cl}^-$   
 203 ions accelerated the carbamazepine degradation rate, in contrast to the scavenging caused by  
 204 nitrate ( $\text{NO}_3^-$ ), sulfate ( $\text{SO}_4^{2-}$ ) and dihydrogen phosphate ( $\text{H}_2\text{PO}_4^-$ ) ions. In fact, 10 mM  $\text{Cl}^-$  enabled  
 205 99% degradation in 1 min, whereas a chloride-free system eliminated 60% of carbamazepine in 10  
 206 min, arguing that this could be caused by the cogeneration of additional chlorine-derived radicals  
 207 [59]. Recently, researchers have also explored the use of novel catalysts based on both iron and  
 208 cobalt for the activation of PMS. Wu et al. (2019) developed cobalt ferrite nanoparticles ( $\text{nCoFe}_2\text{O}_4$ )  
 209 under several supports, of which organo-montmorillonite was found to be particularly promising as  
 210 an inexpensive and effective support material [60]. It exhibited high carbamazepine removal  
 211 efficiencies during three successive cycles (i.e., 73 – 93% degradation and up to  $2.34 \text{ h}^{-1}$  rate  
 212 constant) due to the superior performance of  $\text{Co}^{2+}$  to generate  $\text{SO}_4^{\cdot-}$  radicals, while ensuring less  
 213 than 0.03% toxic cobalt leaching into the effluent [60]. A stable layered double oxide (LDO)-  
 214 supported Co-Fe bimetal catalyst ( $\text{Co}_2\text{FeAl-LDO}$ ) was investigated by Sun et al. (2020), leading to  
 215 complete carbamazepine removal and faster degradation kinetics (i.e., up to  $13.22 \text{ h}^{-1}$ ) due to not  
 216 only the specific catalyst structure but also the synergistic effect of cobalt, iron and aluminium [61].  
 217 Their catalyst was effective up to the fifth cycle (i.e., 88% degradation) with an optimal catalyst dose  
 218 of  $60 \text{ mg L}^{-1}$  and an initial PMS concentration of 0.2 mM, leading to  $0.4 \text{ mg L}^{-1}$  cobalt leaching [61].



221  
222  
223  
224



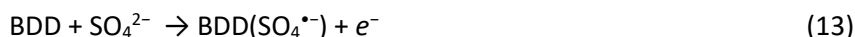
## 225 **2.2 Electrochemical oxidation**

226  
227  
228  
229  
230  
231  
232  
233  
234  
235  
236

Electrochemical oxidation is a popular approach for carbamazepine degradation, although comparison among experimental conditions is a complex matter since they are characterized by multivariate designs, where the material, size and shape of the electrodes, current density, pH, temperature and anolyte composition have all been reported to play a relevant role in the final removal efficiency. Across most studies under review, higher current densities, anolyte and precursor concentrations generally led to higher degradation rates, except for the electro-Fenton treatment because of the iron-related competition reactions [62]. First, the type of electrodes used is a distinguishable feature of electrochemical treatments since their nature directly influences their selectivity and surface reactivity [63].

237  
238  
239  
240  
241  
242  
243  
244  
245  
246  
247  
248  
249  
250  
251  
252  
253  
254  
255  
256  
257  
258  
259

Boron-doped diamond (BDD) electrodes have been reported to be powerful anode materials to generate multiple types of oxidative radicals on their surface, including  $\bullet\text{OH}$  and  $\text{SO}_4^{\bullet-}$ . One of their main advantages is that radicals can be formed without the need for chemical precursors since electron transfer mechanisms directly generate  $\bullet\text{OH}$  from water electrolysis and  $\text{SO}_4^{\bullet-}$  from  $\text{SO}_4^{2-}$  ions (Eqs. 12 and 13). Farhat et al. (2015) compared the effects of sulfate- and nitrate-containing anolytes with a BDD anode, showing that the sulfate-based medium yielded reaction rate constants up to 10-15 times higher for multiple contaminants, even at low initial  $\text{SO}_4^{2-}$  concentrations (i.e., 1.6 mM). In the case of carbamazepine, the reaction rate constant obtained was approximately 29.40  $\text{h}^{-1}$ , whereas under the same experimental conditions, the rate decreased to approximately 2.40  $\text{h}^{-1}$  when  $\text{NaNO}_3$  replaced  $\text{Na}_2\text{SO}_4$  as the anolyte [64]. Song et al. (2018) studied the contribution of BDD electrochemical treatment on PS- and PMS-based AOPs, and in both cases, it was observed that carbamazepine degradation could significantly increase from 0.16  $\text{h}^{-1}$  and 0.21  $\text{h}^{-1}$  with PS and PMS alone, up to 6.81  $\text{h}^{-1}$  and 18.77  $\text{h}^{-1}$  with the added electrochemical oxidation, respectively [65]. Fast carbamazepine degradation using BDD (i.e., 11.34  $\text{h}^{-1}$ ) was also observed by García-Espinoza et al. (2018) in a spiked wastewater effluent when NaCl anolyte was used [27]. García-Espinoza and Nacheva (2019) further investigated the role of the anolyte species by testing BDD performance in the presence of  $\text{Na}_2\text{SO}_4$ , NaCl and NaBr as well as if no additional anolyte is added. Assays revealed that electrochemical oxidation was considerably faster in NaBr and NaCl (i.e., up to 22.81  $\text{h}^{-1}$  and 7.08  $\text{h}^{-1}$ , respectively) than in  $\text{Na}_2\text{SO}_4$  synthetic solutions (i.e., up to 1.23  $\text{h}^{-1}$ ), both with and without oxygen addition [66]. Nonetheless, when applied to a spiked secondary effluent, carbamazepine degradation showed faster kinetics than in the synthetic solution with  $\text{Na}_2\text{SO}_4$  anolyte (i.e., up to 2.75  $\text{h}^{-1}$ ). The rationale behind these results is that the increased matrix complexity enabled the generation of additional oxidants at the anode surface, such as HClO and  $\text{H}_2\text{S}_2\text{O}_8$  [66].



264  
265 Another commonly used electrode material is Ti/PbO<sub>2</sub>, although it has shown slower degradation  
266 kinetics than BDD. García-Espinoza et al. (2016) investigated the performance of Ti/PbO<sub>2</sub> anodes in a  
267 cylindrical mesh shape to promote the production of reactive oxygen species, such as O<sub>3</sub>, H<sub>2</sub>O<sub>2</sub> and  
268  $\cdot\text{OH}$  radicals, obtaining a rate of approximately 0.77 h<sup>-1</sup> [67]. Tran et al. (2017) tested rectangular  
269 Ti/PbO<sub>2</sub> anodes and attained a maximum degradation rate constant of 0.81 h<sup>-1</sup> [68]. Circular Ti/PbO<sub>2</sub>  
270 and BDD anodes were compared by García-Gómez et al. (2014), and in this case, Ti/PbO<sub>2</sub> led to a  
271 slightly higher degradation (i.e., approximately 8% higher), although the attained kinetics were still  
272 similar to other Ti/PbO<sub>2</sub> studies (i.e., 1.26 h<sup>-1</sup>) [63]. Other researchers have also investigated the  
273 performance of alternative electrode materials, such as Ti/Ta<sub>2</sub>O<sub>5</sub>-SnO<sub>2</sub> by Gurung et al. (2018). In  
274 comparison to conventional Ti/PbO<sub>2</sub>, their newly developed anode showed a slightly lower  
275 carbamazepine degradation efficiency (i.e., 71.7% in contrast to 77.9% after 8 h). However, this  
276 material turned out to be more energy-efficient and effective during the treatment of a spiked  
277 membrane bioreactor effluent, while neither leaching heavy metals nor being affected by the pH  
278 [69]. A novel blue-colored TiO<sub>2</sub> nanotube array membrane filter anode was studied by Xu et al.  
279 (2021), which, due to the generation of multiple radical species (i.e., SO<sub>4</sub><sup>·-</sup>,  $\cdot\text{OH}$ , O<sub>2</sub><sup>·-</sup>), showed fast  
280 degradation kinetics up to 24.18 h<sup>-1</sup>. Their study also showed that the presence of Cl<sup>-</sup> enhanced  
281 carbamazepine degradation since additional Cl<sup>·</sup> radicals were formed, whereas NO<sub>3</sub><sup>-</sup> inhibited the  
282 degradation rate because of a set of proposed competition reactions with  $\cdot\text{OH}$  radicals [70]. Finally, a  
283 mediated electrochemical oxidation process based on Co(III) was reported by Liu et al. (2019), where  
284 no radical species were detected and the main oxidizing substance was Co(III) ions, allowing for  
285 complete carbamazepine degradation in 50 min [4, 71].

286  
287 Komtchou et al. (2015) compared electrochemical oxidation with the electro-Fenton process and  
288 electroperoxidation process. In their electro-Fenton study, different types of anode materials were  
289 investigated, where BDD allowed for up to 75% higher carbamazepine degradation and 4-fold higher  
290 TOC removal than Ti/Pt and Ti/SnO<sub>2</sub> [62]. However, it was revealed that the anode selection  
291 significantly affected the underlying degradation mechanisms, as BDD showed a predominant  
292 contribution of direct oxidation of carbamazepine (i.e., corresponding to 36% degradation) in  
293 contrast to electro-Fenton and electroperoxidation (i.e., attributed to 23% and 14% degradation,  
294 respectively). On the other hand, Ti/Pt promoted the electro-Fenton reaction (i.e., 36%  
295 carbamazepine degradation) over electroperoxidation (i.e., 21%) and direct oxidation (i.e., 8.6%)  
296 [62]. In comparison to other studies, the lower degradation percentages attained in the direct  
297 oxidation scenario may be attributed to the considerably lower current density applied.

### 298 299 300 **2.3 Photo(catalytic)oxidation**

301  
302 Carbamazepine degradation by direct photolysis, both in natural and simulated sunlight, has not  
303 been found to be a successful treatment since considerably low degradation rate constants have  
304 been reported (i.e., lower than 0.01 h<sup>-1</sup>) [72–74]. Photolysis in real wastewater effluents has shown  
305 slightly higher degradation rates (i.e., up to 0.022 h<sup>-1</sup>) when additional matrix constituents enabled  
306 indirect photolysis pathways. For instance, the presence of NO<sub>3</sub><sup>-</sup> ions promoted photodegradation  
307 given that it is a photosensitizer, and in contrast, humic acid hindered it since it absorbed part of the

308 available irradiation energy and reformed the parent compound [72]. As a result, photodegradation  
309 treatment has often been studied in combination with oxidant species, such as chlorine, ozone or  
310 hydrogen peroxide, as well as with the Fenton treatment,  $\text{SO}_4^{\bullet-}$  precursors and metal catalysts.

311 Deng et al. (2013) performed a comparative study on the performance of different common  
312 oxidants with UV irradiation, namely, UV/ $\text{H}_2\text{O}_2$ , UV/PMS and UV/PS. Based on energy requirements,  
313 oxidant costs and operating conditions, the UV/PS system was proposed as the most efficient and  
314 economic method with a degradation rate constant up to  $10.83 \text{ h}^{-1}$ . In contrast, UV/ $\text{H}_2\text{O}_2$  and  
315 UV/PMS yielded maximum degradation rate constants of approximately  $7.45 \text{ h}^{-1}$  and  $1.55 \text{ h}^{-1}$ ,  
316 respectively. Experimental results also revealed that increasing the oxidant dose had a positive  
317 influence on the kinetics and that optimal pH conditions were acidic for UV/ $\text{H}_2\text{O}_2$  and UV/PS (i.e., pH  
318 3 and 5, respectively) and basic for UV/PMS (i.e., pH 11). Both UV/ $\text{H}_2\text{O}_2$  and UV/PS were inhibited in  
319 the presence of  $\text{Cl}^-$  and  $\text{CO}_3^{2-}$ , whereas the UV/PMS system showed a degradation increase under  
320 certain conditions [75]. Other studies have also reported high carbamazepine degradation  
321 efficiencies (i.e., over 79% removal) within short reaction times (i.e., from 9 s to 3 min) under the  
322 combined treatment of UV with these oxidants [3, 51, 76]. Additionally, it was found that the  
323 presence of Fe(II) as a catalyst in the UV/PMS and UV/PS systems enhanced the removal efficiency,  
324 reaching almost complete degradation [76]. In another study, the carbamazepine degradation rate  
325 constant under UV/PMS/Fe(II) treatment was reported to reach  $11.21 \text{ h}^{-1}$  [74]. Few studies have also  
326 reported UV/ $\text{O}_3$  as an effective treatment for the removal of carbamazepine [51, 77].  
327

328 Regarding chlorine-based UV methods, Wang et al. (2016) observed that neither UV irradiation  
329 nor chlorination could effectively degrade carbamazepine when applied individually. However, the  
330 combination of both under acidic conditions showed a synergistic effect resulting from the combined  
331 generation of  $\cdot\text{OH}$  and  $\text{Cl}\cdot$  radicals, which allowed for a degradation rate constant of up to  $85.2 \text{ h}^{-1}$ . In  
332 simulated wastewater, the same treatment showed an inhibition of approximately 30% since  
333 dissolved organic matter (DOM) acted as an oxidation consumer and light filter as well as  
334 bicarbonate ions ( $\text{HCO}_3^-$ ) reacted with both  $\cdot\text{OH}$  and  $\text{Cl}\cdot$  to generate carbonate radicals ( $\text{CO}_3^{\bullet-}$ ), which  
335 are milder oxidant species towards organic compounds [78]. Sichel et al. (2011) also previously  
336 reported the potential of UV/chlorine systems from an energy point of view. Their research showed  
337 that 90% carbamazepine degradation could be attained in simulated wastewater at the technical  
338 scale (i.e.,  $250 \text{ L h}^{-1}$  continuous flow reactor), while showing approximately 75% energy reduction  
339 compared to UV/ $\text{H}_2\text{O}_2$  [79].  
340

341 Improving the degradation efficiency in a UV system is possible via the addition of a  
342 photocatalyst such as a semiconductor oxide. In particular,  $\text{TiO}_2$  has been widely investigated  
343 because of its low cost, high stability and activity, abundance, and feasibility for immobilization on  
344 different supports [80]. Franz et al. (2020) compared a heterogeneous  $\text{TiO}_2$  mesh and conventional  
345  $\text{TiO}_2$  powders (i.e., Degussa P25) and reported that carbamazepine degradation rate constants were  
346  $1.08 \text{ h}^{-1}$  and  $10.44 \text{ h}^{-1}$ , respectively. This difference originates from the various active surface areas  
347 of the catalysts, which also led to different UV dosage efficiencies. Nonetheless, even if the  
348 dispersed  $\text{TiO}_2$  powders are more effective, the supported mesh is more easily recovered and  
349 regenerated [80]. Similar degradation kinetics have been observed on other heterogeneous [3, 74,  
350 81, 82] and homogeneous  $\text{TiO}_2$  systems [83], as summarized in Table 1. Other photocatalysts have  
351 also been explored for carbamazepine degradation, such as bismuth-, zinc- and tungsten-derived  
352 oxides. Given that the morphology and optical abilities of these catalysts directly influence  
353 adsorption and reaction mechanisms taking place, the results on carbamazepine removal are  
354 diverse. Under specific conditions, monoclinic- $\text{BiPO}_4$  and triclinic- $\text{WO}_3$  photocatalysts have reported  
355 degradation rate constants up to  $7.86 \text{ h}^{-1}$  and  $7.64 \text{ h}^{-1}$ , respectively [84, 85]. The highest degradation  
356 rate constant has been reported in acidic synthetic wastewater when using  $\text{BiOCl}_{0.875}\text{Br}_{0.125}$ , achieving

357 a value of 25.80 h<sup>-1</sup> [83]. In the case of ZnO nanoparticles, photodegradation of carbamazepine has  
358 shown slower kinetics (i.e., 0.84 h<sup>-1</sup>), coupled with reduced photocatalytic activity due to the  
359 photocorrosion of ZnO in aqueous solutions [81]. Finally, photo-Fenton treatment has also been  
360 explored for the degradation of carbamazepine in wastewater treatment [3, 56]. In the work by  
361 Klammerth et al. (2010), the solar photo-Fenton treatment displayed a degradation rate constant up  
362 to 0.84 h<sup>-1</sup> even at low iron and H<sub>2</sub>O<sub>2</sub> concentrations, although its performance was affected by the  
363 presence of <sup>•</sup>OH radical scavengers such as CO<sub>3</sub><sup>2-</sup>. A main limiting factor for the application of this  
364 photo-Fenton system in real wastewater was that tests with *Vibrio fischeri* showed that the  
365 generated degradation products led to a toxicity increase [56].  
366

### 367 **3 Advanced reduction processes**

369 Advanced reduction processes (ARPs) operate in an opposite manner to AOPs, as they rely on the  
370 formation of highly reactive reducing radicals, such as hydrated electrons (e<sub>aq</sub><sup>-</sup>), hydrogen atoms  
371 (H<sup>•</sup>), sulfite radicals (SO<sub>3</sub><sup>•-</sup>) and sulfur dioxide radicals (SO<sub>2</sub><sup>•-</sup>), to degrade oxidized compounds [41,  
372 86]. In particular, ARPs have been applied to the degradation of persistent per- and polyfluoroalkyl  
373 substances (PFAS), as already shown in the state-of-the-art review by Cui et al. (2020), where the  
374 chemical mechanisms behind several types of ARPs are discussed [86]. Regarding the degradation of  
375 carbamazepine, Yu et al. (2021) investigated for the first time its removal in a UV/sulfite ARP.  
376 Experimental results showed synergistic effects, where 99.6% carbamazepine degradation was  
377 attained after 30 min (i.e., with a degradation rate constant of 20.4 h<sup>-1</sup>), in contrast to the  
378 nonsignificant degradation efficiencies observed when sulfite and UV were used independently [40].  
379 The degradation rate constant was found to increase with increasing sulfite concentration, UV  
380 irradiance and pH, attaining optimal values under alkaline conditions since e<sub>aq</sub><sup>-</sup> was the dominant  
381 reductive species [40].  
382

### 383 **4 Biological treatments**

384  
385  
386 Biological wastewater treatments rely on the degradation of contaminants by the metabolism of  
387 microbial cultures. For the degradation of carbamazepine, conventional activated sludge (CAS)  
388 processes alone or in combination with membrane bioreactors (MBR) have been investigated, where  
389 the former entail a settling tank to separate the formed sludge and the latter are based on sludge  
390 separation via microfiltration or ultrafiltration membranes [33]. In both treatments, almost  
391 negligible carbamazepine degradation efficiencies have been observed (i.e., typically below 10%)  
392 [26]. These poor results are attributed to carbamazepine's moderate hydrophilicity (i.e., logP = 2.45),  
393 low water-sludge distribution coefficient (i.e., 1.2 L kg<sub>ss</sub><sup>-1</sup>), and the presence of an electron  
394 withdrawing functional group (i.e., amide group) in its structure, which increases the biodegradation  
395 resistance [33]. Higher degradation efficiencies have been attained by Tahir et al. (2021) by  
396 selectively enriching wastewater with sulfate-reducing and fermentative acidogenic bacteria. After  
397 144 h, their anaerobic bioreactor yielded 46% carbamazepine degradation, coupled with 36% total  
398 organic carbon (TOC) removal, 98% sulfate (SO<sub>4</sub><sup>2-</sup>) reduction and the production of several volatile  
399 fatty acids (i.e., acetic acid, propionic acid and butyric acid) [87]. In addition, under these conditions,  
400 the degradation of carbamazepine was higher than that in a mixed microbial community (i.e., 36%),  
401 and the enriched microbial community was more resistant to the toxicity resulting from increased  
402 carbamazepine concentrations [87]. In a different study, carbamazepine degradation was enhanced  
403

404 by the combination of activated sludge and gamma irradiation in a two-step treatment, leading up to  
405 99.8% carbamazepine removal and 79.3% mineralization when 800 Gy irradiation was applied [88].  
406

407 As an alternative to bacterial-dominated activated sludge processes, white-rot fungi have been  
408 found to be more effective in degrading recalcitrant compounds due to the generation of  
409 extracellular and intracellular enzymes, the latter being more suitable to target the amide group in  
410 the carbamazepine structure [33]. Nonetheless, attained efficiencies have been observed to be  
411 dependent on the fungal species and subsequent enzymes as well as on the need for operation  
412 under sterile conditions to avoid bacterial contamination [33]. In the treatment investigated by Hata  
413 et al. (2010), carbamazepine was treated with ligninolytic enzymes (i.e., laccase and manganese  
414 peroxidase). In their work, they showed that there was no significant carbamazepine degradation if  
415 laccase alone was used, whereas manganese peroxidase allowed for 14% elimination after one cycle  
416 of 24 h. In the presence of laccase with a redox mediator (i.e., 1-hydroxybenzotriazole), a single  
417 treatment cycle led to 22% removal in 24 h, and repeated 8-h cycles for a period of 48 h showed 60%  
418 elimination [89]. In the presence of crude lignin peroxidase, other studies reported less than 15%  
419 elimination after 2 h [90]. The highest removal efficiencies have been observed through specific  
420 whole-cell white-rot fungi under sterile conditions, where multiple enzymes are generated [33]. For  
421 instance, species such as *Bjerkandera* sp. R1, *Bjerkandera adusta* and *Pleurotus ostreatus* (PC9)  
422 allowed for 99% removal in a span of 14 to 32 incubation days [91, 92]. Nevertheless, lower  
423 efficiencies have also been observed (i.e., less than 60% elimination) for several white-rot fungal  
424 cultures under different operating conditions [33, 93].  
425  
426

## 427 5 Physical treatments

428  
429 Activated carbon (AC) is a well-established material used in adsorption processes because of its high  
430 porosity, surface area and affinity to interact with a wide range of compounds, eventually retaining  
431 them on its surface [3, 94]. It is typically used in either powdered or granular form, referred to as PAC  
432 and GAC, respectively [95, 96]. Given that carbamazepine is considered an adsorbable compound  
433 that stays in neutral form regardless of the operating pH, it has been found to be suitable for AC  
434 separation [33, 97]. Under PAC, over 90% removal effectiveness has been reported, even if low  
435 carbon doses were used [3]. In the same study, a GAC bed reactor enabled the removal of 72%  
436 carbamazepine in 23,400 bed volumes [3]. The difference between both methods lies in the fact that  
437 PAC has a larger specific surface area for removal [33]. More recently, metal-organic framework  
438 (MOF)-derived nanoporous carbons have attracted growing interest as adsorbents because of their  
439 high porosity, specific surface area and chemical stability [98, 99]. In the study by Yu et al. (2022),  
440 MOF-5 showed a higher adsorption capacity and faster uptake rate than ZIF-8-derived nanoporous  
441 carbon and commercial PAC for the removal of carbamazepine, with the graphitic defects being the  
442 key feature to improve the adsorption [99]. Their MOF-5 could be reused for 5 cycles, attaining  
443 removal efficiencies higher than 87% [99]. Other recently developed adsorbents with a maximum  
444 capacity for carbamazepine adsorption ranging from approximately 208 to 286 mg g<sup>-1</sup> are activated  
445 palm kernel shell [100], zirconia/porous carbon nanocomposites [101], hierarchically structured  
446 carbon composites [102] and biomass activated carbon [103], which are comparable to the  
447 adsorption capacity of commercial PAC (i.e., 225 – 274 mg g<sup>-1</sup>) [100, 104].

448 Regarding membrane filtration in wastewater treatment, pollutant removal relies on the  
449 effectiveness of a pressure-driven physical barrier to impede the passage of target compounds and  
450 hence separating contaminants from the influent. In wastewater treatment facilities at a large scale,

nanofiltration (NF) and reverse osmosis (RO) are the most commonly used types [3]. In terms of carbamazepine separation, Radjenovic et al. (2008) reported carbamazepine rejection percentages higher than 97% and 99% when NF and RO membranes were used, respectively [105]. Hai et al. (2018) also reviewed available studies on carbamazepine removal via NF and RO, showing that the final efficiency was strongly dependent on the molecular weight cut-off (MWCO) of the membranes and their fouling [33].

Both adsorption and filtration systems are essentially separation methods that do not entail degradation mechanisms, and consequently, they need to be coupled with an additional unit to carry out pollutant elimination, typically through advanced oxidation processes. Nonetheless, both are useful techniques to reduce the wastewater volume to be further treated and hence minimize the need for large-scale operations.

## 6 Hybrid treatments

The purpose of hybrid processes is to combine multiple wastewater treatment methods to promote a synergistic effect that can enhance pollutant degradation. To this end, carbamazepine degradation has been explored under sonoelectrooxidation [68], sono-Fenton [106], radiolysis/H<sub>2</sub>O<sub>2</sub> [31], photoelectrocatalysis [80, 107] and UV/PS/Fe(II)/US/H<sub>2</sub>O<sub>2</sub> treatments [108].

Tran et al. (2017) investigated the performance of an electrochemical cell in combination with ultrasound, where Na<sub>2</sub>SO<sub>4</sub> was used as the anolyte and Ti/PbO<sub>2</sub> and Ti were used as the anode and cathode, respectively. Their results revealed that the degree of synergy increased with decreasing current intensity and increasing ultrasound power. After 30 days of treatment, the observed carbamazepine degradation percentage (i.e., 99.5%) was higher than that with electrolysis alone (i.e., 91%). In this setup, the maximum reported degradation rate constant corresponded to ca. 0.76 h<sup>-1</sup> [68]. Ultrasound technology has also been investigated in combination with the Fenton process by Ghauch et al. (2011), where low frequency ultrasound irradiation was dedicated to cleaning the iron catalyst due to corrosion. Recycling experiments showed that reused iron catalysts could promote the satisfactory degradation of carbamazepine (i.e., up to 85% per cycle) after 4 successive cycles [106]. Similar to the conventional Fenton reaction, the degradation efficiency of the US/Fe(0)/H<sub>2</sub>O<sub>2</sub> system is strongly dependent on the acidic nature of the solution [106]. Liu et al. (2016) demonstrated that electron beam radiolytic treatment combined with H<sub>2</sub>O<sub>2</sub> addition could further promote carbamazepine degradation and mineralization since both oxidative and reductive species could be generated simultaneously. It was also reported that the addition of H<sub>2</sub>O<sub>2</sub> contributed to the decomposition of some mutagenic and carcinogenic transformation products [31].

Regarding photoelectrocatalytic treatments, Dagher et al. (2013) carried out a comparative study on carbamazepine degradation utilizing Ti/TiO<sub>2</sub> nanostructured electrodes in combination with cathodes of different natures. Optimal degradation was observed with a vitreous carbon cathode, reaching up to 73.5% degradation (i.e., 0.24 h<sup>-1</sup> reaction rate constant) and 21.2% mineralization after 120 min [107]. Faster degradation kinetics were reported by Franz et al. (2020) when using TiO<sub>2</sub> meshes in photoelectrocatalysis (i.e., 4.56 h<sup>-1</sup>). In fact, when combining photocatalysis with electrochemical treatment, an increase by a factor of 4.2 was observed with respect to heterogeneous photocatalysis on a supported TiO<sub>2</sub> mesh [80]. As previously discussed in section 2.3, conventional photocatalysis with commercial Degussa P25 TiO<sub>2</sub> powders was in this study more

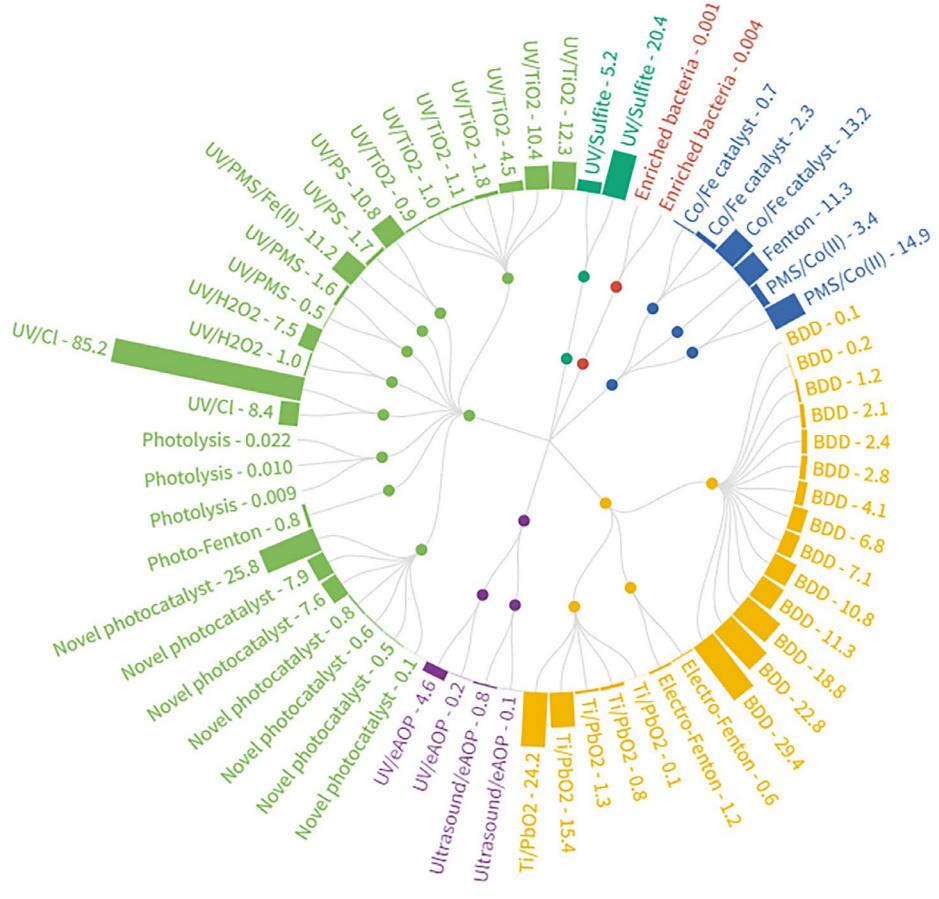
499 effective (i.e., 10.44 h<sup>-1</sup>) than the photoelectrocatalytic treatment, although powdered catalyst  
500 presents the drawback of a more complex recovery at the industrial scale [80].  
501

502 Finally, a more extensive hybrid system was proposed by Monteagudo et al. (2015), which was  
503 dedicated to the simultaneous activation of PS by Fe<sup>2+</sup> ions, thermal energy, ultrasound and UV  
504 irradiation, in addition to the catalytic activity of Fe<sup>2+</sup> on H<sub>2</sub>O<sub>2</sub> decomposition under acidic conditions.  
505 In contrast to the mineralization efficiencies observed in isolated or binary combinations of these  
506 methods (i.e., less than 26.4% TOC removal), the hybrid setup could reach 99% mineralization [108].  
507 This study revealed that the presence of sulfate electrolytes inhibited the coalescence of cavitation  
508 bubbles and increased the concentration of SO<sub>4</sub><sup>•-</sup> radicals. In addition, the iron catalyst could be  
509 regenerated through UV irradiation [108].  
510

## 511 **7 Opportunities and limitations**

513 Conventional physical and biological treatments are not considered stand-alone solutions to degrade  
514 carbamazepine. The former is a separation process that requires further treatment, and the latter  
515 typically entails considerably slow kinetics (i.e., less than 0.004 h<sup>-1</sup>) to eventually attain minor or  
516 negligible carbamazepine degradation efficiencies (Table 2). Nonetheless, both can help increase the  
517 efficiency of other treatments, such as AOPs. Physical treatments preconcentrate wastewater and  
518 hence reduce the reactor volume needed and its derived operational costs, while biological  
519 treatments enhance mineralization efficiencies by targeting biodegradable compounds in the  
520 effluent. Likewise, and despite the successful kinetics observed in the UV/sulfite system (i.e.,  
521 between 5.2 and 20.4 h<sup>-1</sup>), ARPs for carbamazepine degradation have not been extensively  
522 investigated, as shown by the limited number of available research articles (Table 2). Consequently,  
523 additional studies are needed to evaluate their strengths and pitfalls as well as their suitability for  
524 industrial applications.  
525

526 As reflected in Table 1 and Figure 2, the possibilities for further implementation of AOPs are more  
527 extensive. Most treatments can be found within a window of 4 to 12 h<sup>-1</sup> degradation rate constant  
528 (Fig. 3), meaning that 99% carbamazepine removal can be attained in a time span between 20 to 70  
529 min. The largest body of literature is dedicated to UV-based treatments, which range from the low  
530 kinetics attained via photolysis alone (i.e., less than 0.03 h<sup>-1</sup>) up to the notably higher degradation  
531 rates observed in UV/chlorine systems (i.e., up to 85.2 h<sup>-1</sup>). However, before taking the leap towards  
532 the industrial implementation of UV-based treatments, not only the degradation effectiveness of a  
533 single study is the key parameter to take into consideration. In the case of UV/chlorine treatment, it  
534 is essential to optimize chlorine dosages and mitigate scavenging effects in complex wastewater  
535 matrices, such as those caused by DOM and HCO<sub>3</sub><sup>-</sup> ions. In addition, it is imperative to quantify the  
536 risks of increased effluent toxicity since the presence of Cl<sup>-</sup> ions in wastewater can further lead to  
537 the production of species such as chlorate (ClO<sub>3</sub><sup>-</sup>) and perchlorate (ClO<sub>4</sub><sup>-</sup>). Other combinations of UV  
538 and chemical precursors, such as PS, PMS and the Fenton reaction, have reported either similar or  
539 lower rates in comparison to their chemical-based counterparts. This evidence indicates that the  
540 development of hybrid treatments should also be closely evaluated. It is commonly assumed that  
541 synergistic effects are intrinsic to hybrid setups, although as seen in the case of carbamazepine  
542 degradation (Fig. 2), considerably slower degradation kinetics can also be triggered.  
543  
544  
545  
546



Treatment ● ARPs ● Biological ● Chemical ● eAOPs ● Hybrid ● UV-based

Figure 2: Carbamazepine degradation rates for several wastewater treatments. The height of the bars corresponds to the value of the pseudo-first order kinetic constant ( $h^{-1}$ ) reported in a specific literature reference.

548

549

550

551

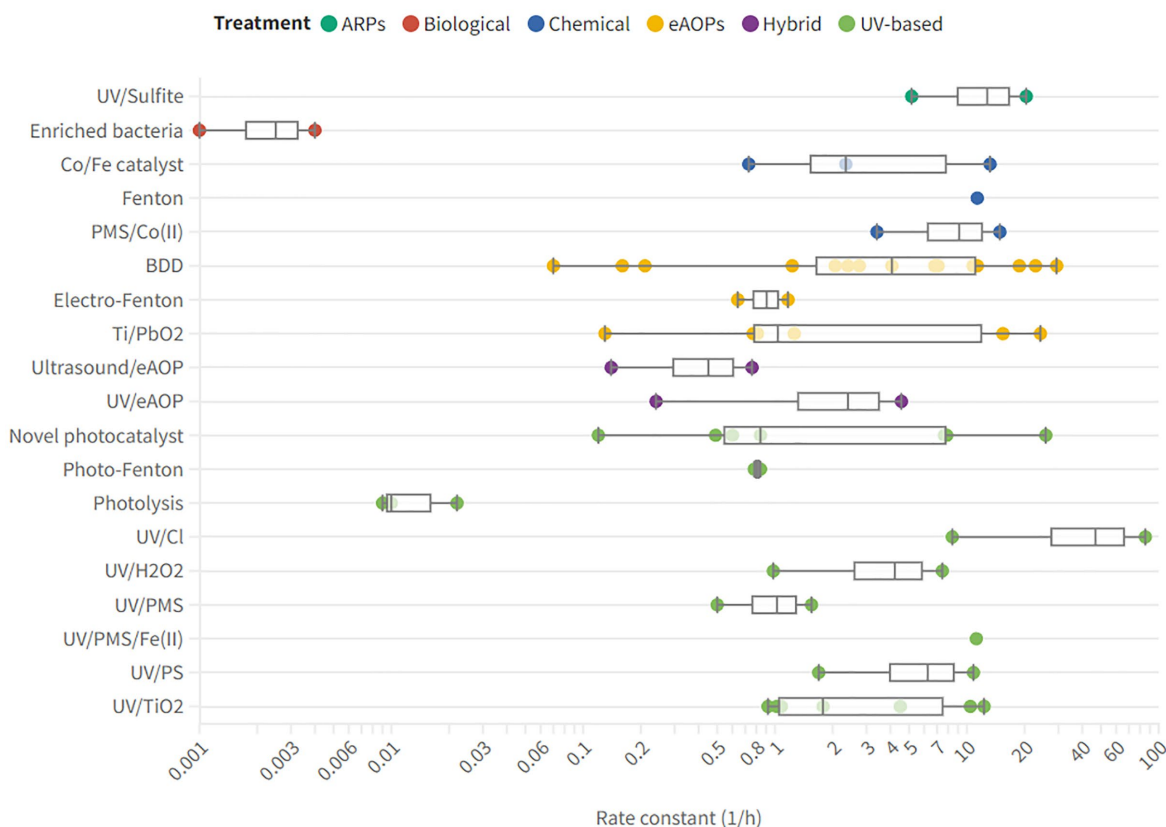


Figure 3: Average carbamazepine degradation rates ( $\text{h}^{-1}$ ) for several wastewater treatments.

Chemically activated AOPs, such as ozonation, Fenton process and sulfate radical precursor-based oxidation, have been reported to be effective for carbamazepine degradation (Table 1), although they also pose several advantages and limitations for future industrial applications. Ozonation presents the advantages of operating under mild conditions while leading to high removal percentages (i.e., close to 100%). However, the use of ozone is costly, yields low mass transfer efficiencies and utilization rates during the AOP treatment, and is strongly influenced by suspended solids and organic matter. The formation of bromate through ozonation also adds as a constraint that the use of wastewater containing  $\text{Br}^-$  ions should be avoided or pretreated. Fenton treatments are easy to operate and provide high degradation kinetics (i.e.,  $11.3 \text{ h}^{-1}$ ); although a low pH is needed, iron catalyst consumption and the co-production of large amounts of iron sludge hinder its application in continuous industrial setups. Sulfate radical-based AOPs that rely on PMS and PS present high degradation efficiencies (i.e., up to  $14.9 \text{ h}^{-1}$ ) and can be applied to a wide range of wastewater since the advantages of both  $^{\bullet}\text{OH}$  and  $\text{SO}_4^{\bullet-}$  radicals can be exploited depending on the application at hand. The drawbacks of these treatments are not only the need for considerable amounts of chemical precursors but also the associated potential increase in sulfate residuals and acidity of the treated effluents. To overcome these limitations, subsequent posttreatment should be implemented, which also increases the overall operational costs. These chemical-based AOPs also have in common that they typically rely on the catalytic generation of oxidative radicals, where the implications of applying homogeneous or heterogeneous catalysts are quite diverse. Homogeneous catalysts are burdensome to recover, and hence it is complicated to prevent the leaching of metals and catalyst components into effluents. On the other hand, heterogeneous catalysts mitigate these leaching effects, but catalyst reuse remains a challenging matter. As a result, heterogeneous catalysts are preferred and typically implemented in the form of magnetic nanoparticles, although it

579 is necessary to further improve their reusability while decreasing their production costs.

580

581 Based on the reviewed literature (Table 1), electrochemical and photocatalytic AOPs have  
582 consistently reported effective carbamazepine degradation results, more specifically,  
583 electrochemical treatments driven by the use of boron-doped diamond (BDD) or Ti/PbO<sub>2</sub> anodes and  
584 photocatalytic treatments involving TiO<sub>2</sub> or novel photocatalysts. The maximum degradation  
585 efficiencies attained by BDD electrodes, Ti/PbO<sub>2</sub> electrodes and novel photocatalysts oscillate  
586 between 24.2 and 29.4 h<sup>-1</sup> under optimal conditions, with the TiO<sub>2</sub> photocatalysts being slightly less  
587 efficient (i.e., up to 12.3 h<sup>-1</sup>). Nonetheless, degradation rate constants as low as 0.1 h<sup>-1</sup> have also  
588 been observed for these treatments when the presence of radical scavengers has played a major  
589 hindering role. The added value of these technologies is that effective carbamazepine degradation  
590 can be attained under mild operating conditions and with minimal or no addition of chemicals to  
591 generate oxidative radicals. In addition, the use of renewable energies contributes to a reduction in  
592 operational costs and environmental impacts. On the other hand, both electrochemical and  
593 photocatalytic treatments showcase limited energy use efficiencies, either in the form of electricity  
594 or light, respectively, which need to be further optimized. In light of a possible future  
595 implementation, other main limitations to be overcome for these AOPs are the high costs that  
596 advanced electrodes and photocatalysts entail, the need for reducing their performance variability  
597 due to wastewater composition effects and the potential formation of toxic byproducts.

**Table 1:** Summary of reported carbamazepine (CBZ) degradation in AOPs for wastewater treatment.

Treatment	Matrix	Initial CBZ (mg L <sup>-1</sup> )	Removal	Rate constant	Comments	Ref.	
Chemical oxidation	Ozonation	Synthetic and Spiked WWTP effluent	1	60 – 99%	-	• O <sub>3</sub> flow: 2.6 g h <sup>-1</sup>	[51]
		Spiked river effluent	5·10 <sup>-4</sup>	100%	-	• pH: 7.3 • [O <sub>3</sub> ]: 0.006 mM	[50]
		WWTP effluent	-	97 – 100%	-	• [O <sub>3</sub> ]: 0.61 ± 0.04 g/g DOC	[3]
	Fenton	Synthetic and WWTP effluent	11.81	7 – 83%	11.34 h <sup>-1</sup>	• pH: 3 • [H <sub>2</sub> O <sub>2</sub> ]: 0.15 – 0.25 mM • [Fe(II)]: 0.15 – 0.25 mM	[54]
		WWTP effluent	1·10 <sup>-3</sup>	100%	-	• pH: 3 • [H <sub>2</sub> O <sub>2</sub> ]: 0.895 mM • [Fe(II)]: 0.358 mM	[55]
		WWTP effluent	0.1	6.6 – 18%	-	• pH: 3 • [H <sub>2</sub> O <sub>2</sub> ]: 0.147 – 1.470 mM • [Fe]: 0.09 mM	[56]
	Fenton/PS	Synthetic	50	77%	-	• pH: 6.8 • [H <sub>2</sub> O <sub>2</sub> ]: 0.5 mM • [PS]: 1 mM • [nZVI]: 2 mM	[57]
	PMS/Co(II)	Synthetic and WWTP effluent	11.81	50 – 100%	3.40 – 14.87 h <sup>-1</sup>	• pH: 3 • [PMS]: 0.15 – 0.25 mM • [Co(II)]: 0.15 – 0.25 mM	[54]
	PS/Fe(II)	Synthetic	5.91	3 – 99%	-	• pH: 2 – 7.87 • [Fe(II)]: 0.05 – 0.75 mM • [PS]: 0.125 – 1.5 mM • [Cl <sup>-</sup> ]: 0 – 10 mM	[59]
	Other catalysts	Synthetic	5	93%	2.34 h <sup>-1</sup>	• pH: 6.8 • Organo-montmorillonite supported nCoFe <sub>2</sub> O <sub>4</sub> catalyst compared with other supports • [nCoFe <sub>2</sub> O <sub>4</sub> /OMt]: 0.4 g L <sup>-1</sup> • [PMS]: 0.5 mM	[60]

		Synthetic	5 – 20	29 – 100%	0.73 – 13.22 h <sup>-1</sup>	<ul style="list-style-type: none"> <li>• pH: 4 – 10</li> <li>• Layered double oxide-supported Co-Fe bimetal catalysts</li> <li>• [Co<sub>2</sub>FeAl-LDO]: 20 – 80 mg L<sup>-1</sup></li> <li>• [PMS]: 0.05 – 0.4 mM</li> </ul>	[61]
Electrochemical oxidation	BDD anodes	Synthetic	0.47	100%	29.40 ± 2.10 h <sup>-1</sup>	<ul style="list-style-type: none"> <li>• pH: 2</li> <li>• Current density: 200 A m<sup>-2</sup></li> <li>• Electrolyte: Na<sub>2</sub>SO<sub>4</sub> (40 mM)</li> </ul>	[64]
		Synthetic	0.47	100%	2.40 ± 0.37 h <sup>-1</sup>	<ul style="list-style-type: none"> <li>• pH: 2</li> <li>• Current density: 200 A m<sup>-2</sup></li> <li>• Electrolyte: NaNO<sub>3</sub> (60 mM)</li> </ul>	[64]
		Synthetic	12	8.6 – 36%	-	<ul style="list-style-type: none"> <li>• pH: 3</li> <li>• Current density: 18 A m<sup>-2</sup></li> <li>• Electrolyte: Na<sub>2</sub>SO<sub>4</sub> (7 mM)</li> </ul>	[62]
		Synthetic	10	82%	0.07 – 1.23 h <sup>-1</sup>	<ul style="list-style-type: none"> <li>• pH: 4</li> <li>• Current density: 403.23 A m<sup>-2</sup></li> <li>• Electrolyte: Na<sub>2</sub>SO<sub>4</sub> (7 mM)</li> <li>• With and without O<sub>2</sub> addition</li> </ul>	[4, 66]
		Synthetic	10	-	4.07 – 7.08 h <sup>-1</sup>	<ul style="list-style-type: none"> <li>• pH: 4</li> <li>• Current density: 403.23 A m<sup>-2</sup></li> <li>• Electrolyte: NaCl (7 mM)</li> <li>• With and without O<sub>2</sub> addition</li> </ul>	[4, 66]
		Synthetic	10	-	10.78 – 22.81 h <sup>-1</sup>	<ul style="list-style-type: none"> <li>• pH: 4</li> <li>• Current density: 403.23 A m<sup>-2</sup></li> <li>• Electrolyte: NaBr (7 mM)</li> <li>• With and without O<sub>2</sub> addition</li> </ul>	[4, 66]
		Synthetic	1.18	-	0.16 – 6.81 h <sup>-1</sup>	<ul style="list-style-type: none"> <li>• Current density: 0 – 100 A m<sup>-2</sup></li> <li>• Electrolyte: NaClO<sub>4</sub> (50 mM)</li> <li>• [PS]: 0 – 5 mM</li> </ul>	[65]
		Synthetic	1.18	-	0.21 – 18.77 h <sup>-1</sup>	<ul style="list-style-type: none"> <li>• Current density: 0 – 100 A m<sup>-2</sup></li> <li>• Electrolyte: NaClO<sub>4</sub> (50 mM)</li> <li>• [PMS]: 0 – 5 mM</li> </ul>	[65]
		Spiked IW effluent	10	100%	2.06 – 2.75 h <sup>-1</sup>	<ul style="list-style-type: none"> <li>• Current density: 403.23 A m<sup>-2</sup></li> <li>• No electrolyte addition</li> <li>• With and without O<sub>2</sub> addition</li> </ul>	[66]
		Spiked WWTP effluent	10	88.7%	11.34 h <sup>-1</sup>	<ul style="list-style-type: none"> <li>• pH: 2</li> <li>• Current density: 161.29 A m<sup>-2</sup></li> <li>• Electrolyte: NaCl (14 mM)</li> </ul>	[27]

Ti-based anodes	Synthetic	2 – 30	53 – 80.3%	0.47 – 1.57 M <sup>-1</sup> s <sup>-1</sup>	<ul style="list-style-type: none"> <li>• Ti/Ta<sub>2</sub>O<sub>5</sub>-SnO<sub>2</sub> and Ti/PbO<sub>2</sub> anodes</li> <li>• pH: 2 – 10</li> <li>• Current density: 10 – 170 A m<sup>-2</sup></li> <li>• Electrolyte: Na<sub>2</sub>SO<sub>4</sub> (100 mM)</li> </ul>	[69]
	Synthetic	10	45.4 – 83.9%	0.77 h <sup>-1</sup>	<ul style="list-style-type: none"> <li>• Ti/PbO<sub>2</sub> cylindrical mesh anode</li> <li>• pH: 7</li> <li>• Current density: 24.1 – 241.5 A m<sup>-2</sup></li> <li>• Electrolyte: Na<sub>2</sub>SO<sub>4</sub> (7 mM)</li> <li>• Pure O<sub>2</sub> addition at 0 – 3 L min<sup>-1</sup></li> </ul>	[67]
	Synthetic	10	-	0.13 – 0.81 h <sup>-1</sup>	<ul style="list-style-type: none"> <li>• Ti/PbO<sub>2</sub> anode</li> <li>• pH: 6.9 – 7.4</li> <li>• Current density: 909 – 13,636 A m<sup>-2</sup></li> <li>• Electrolyte: Na<sub>2</sub>SO<sub>4</sub> (10 mM)</li> </ul>	[68]
	Synthetic	10	53.5 – 89.9%	1.26 h <sup>-1</sup>	<ul style="list-style-type: none"> <li>• Ti/PbO<sub>2</sub> and Ti/BDD anodes</li> <li>• pH: 7</li> <li>• Current intensity: 1 – 2 A</li> <li>• Electrolyte: Na<sub>2</sub>SO<sub>4</sub> (2.82 mM)</li> <li>• Energy: 11.300 – 80.379 kWh m<sup>-3</sup></li> </ul>	[63]
	Synthetic	10	99%	15.42 – 24.18 h <sup>-1</sup>	<ul style="list-style-type: none"> <li>• Blue-colored TiO<sub>2</sub> nanotube arrays membrane filter anode</li> <li>• Current density: 10 – 100 A m<sup>-2</sup></li> <li>• Electrolyte: Na<sub>2</sub>SO<sub>4</sub> (10 mM)</li> <li>• Energy: 0.0246 – 0.6489 kWh m<sup>-3</sup></li> </ul>	[70]
	Synthetic	5	98%	-	<ul style="list-style-type: none"> <li>• Ti/Pt anode</li> <li>• pH: 5.5</li> <li>• Current density: 140 A m<sup>-2</sup></li> <li>• Electrolyte: Na<sub>2</sub>SO<sub>4</sub> (25 mM)</li> </ul>	[4, 71]
	Spiked MBR effluent	0.01	100%	-	<ul style="list-style-type: none"> <li>• Ti/Ta<sub>2</sub>O<sub>5</sub>-SnO<sub>2</sub> anode</li> <li>• pH: 6</li> <li>• Current density: 90 A m<sup>-2</sup></li> <li>• Electrolyte: Na<sub>2</sub>SO<sub>4</sub> (0 – 100 mM)</li> </ul>	[69]
	Electro-Fenton	Synthetic	12 ± 2	29 – 73%	0.64 – 1.17 h <sup>-1</sup>	<ul style="list-style-type: none"> <li>• Nb/BDD, Ti/Pt and TiSn<sub>2</sub> anodes</li> <li>• pH: 3</li> <li>• Current density: 18 – 177 A m<sup>-2</sup></li> <li>• [Fe<sup>+</sup>]: 0 – 0.75 mM</li> <li>• Electrolyte: Na<sub>2</sub>SO<sub>4</sub> (7 mM)</li> </ul>

	Electro-peroxidation	Synthetic	12	30 – 50%	-	<ul style="list-style-type: none"> <li>• Nb/BDD and Ti/Pt anodes</li> <li>• pH: 3</li> <li>• Current density: 18 A m<sup>-2</sup></li> <li>• Electrolyte: Na<sub>2</sub>SO<sub>4</sub> (7 mM)</li> </ul>	[62]
Hybrid processes	Activated sludge/Gamma irradiation	WWTP effluent	17	91.8 – 99.8%	-	<ul style="list-style-type: none"> <li>• 300 – 800 Gy irradiation</li> </ul>	[88]
	Sonoelectro-oxidation	Synthetic	10	24.9 – 81.3%	0.14 – 0.76 h <sup>-1</sup>	<ul style="list-style-type: none"> <li>• Ti/PbO<sub>2</sub> anode</li> <li>• pH: 6.9 – 7.4</li> <li>• Current density: 909 – 1,3636 A m<sup>-2</sup></li> <li>• US Power: 20 – 40 W</li> <li>• Electrolyte: Na<sub>2</sub>SO<sub>4</sub> (10 mM)</li> </ul>	[68]
	Sono-Fenton	Synthetic	9.92	12 – 95%	-	<ul style="list-style-type: none"> <li>• pH: 3 – 9</li> <li>• US frequency: 40 kHz</li> <li>• [Fe(0)]: 0.44 – 3.57 mM</li> <li>• [H<sub>2</sub>O<sub>2</sub>]: 12.5 – 100 mM</li> </ul>	[106]
	UV/PS/Fe(II)/US/H <sub>2</sub> O <sub>2</sub>	Synthetic	15	87.7 – 99%	-	<ul style="list-style-type: none"> <li>• pH: 2.8</li> <li>• UV irradiation: 7.81·10<sup>-6</sup> E s<sup>-1</sup></li> <li>• US amplitude: 100%</li> <li>• [PS]: 300 – 900 mg L<sup>-1</sup></li> <li>• [Fe(II)]: 5 – 15 mg L<sup>-1</sup></li> <li>• [H<sub>2</sub>O<sub>2</sub>]: 100 mg L<sup>-1</sup></li> </ul>	[108]
	Radiolysis/H <sub>2</sub> O <sub>2</sub>	Synthetic	75	100%	0.77 – 2.63 kGy <sup>-1</sup>	<ul style="list-style-type: none"> <li>• 1.8 MeV and 0 – 10 mA electron beam</li> <li>• Irradiation doses: 0.5 – 20 kGy</li> <li>• [H<sub>2</sub>O<sub>2</sub>]: 0 – 200 mM</li> </ul>	[31]
	Photoelectro-catalysis	Synthetic	10 – 20	21.6 – 73.5%	0.24 h <sup>-1</sup> 2.36 M <sup>-1</sup> s <sup>-1</sup>	<ul style="list-style-type: none"> <li>• Ti/TiO<sub>2</sub> anode, and SS, Gr, VC, a-C1 and a-C2 cathodes</li> <li>• pH: 5.5 – 7.3</li> <li>• Current density: 2.7 – 33.6 A m<sup>-2</sup></li> <li>• UV irradiation: 69 W m<sup>-2</sup></li> <li>• Electrolyte: Na<sub>2</sub>SO<sub>4</sub> (50 mM)</li> </ul>	[107]
		Synthetic	0.1	99%	4.56 ± 0.12 h <sup>-1</sup>	<ul style="list-style-type: none"> <li>• TiO<sub>2</sub> mesh anode</li> <li>• Potential: 122.1 V m<sup>-2</sup></li> <li>• UV irradiation: 916 W m<sup>-2</sup></li> <li>• Energy: 7.58 kWh m<sup>-3</sup></li> </ul>	[80]
Photodegradation	Photolysis	Synthetic	0.15	50%	0.009 ± 0.0007 h <sup>-1</sup>	<ul style="list-style-type: none"> <li>• Natural sunlight</li> <li>• pH: 8.0 ± 0.1</li> <li>• Solar irradiance: 7.7 – 9.2 kW m<sup>-2</sup></li> </ul>	[72]

	Synthetic	9.5	15 – 100%	0.01 – 1.30 h <sup>-1</sup>	<ul style="list-style-type: none"> <li>• Simulated sunlight</li> <li>• pH: 2.9 – 9.0</li> <li>• Not sparged, sparged with O<sub>2</sub> and sparged with N<sub>2</sub></li> <li>• Solar irradiance: 55 W m<sup>-2</sup></li> </ul>	[73]
	WWTP effluent	11.81	8%	-	<ul style="list-style-type: none"> <li>• Simulated sunlight</li> <li>• pH: 7.8</li> <li>• Photonic flux: 7.9·10<sup>6</sup> E min<sup>-1</sup></li> </ul>	[74]
	WWTP effluent	0.15	50%	0.022 ± 0.014 h <sup>-1</sup>	<ul style="list-style-type: none"> <li>• Natural sunlight</li> <li>• pH: 7.85 ± 0.21</li> <li>• Solar irradiance: 7.7 – 9.2 kW m<sup>-2</sup></li> </ul>	[72]
UV/Chlorine	Synthetic	2	98%	8.4 – 85.2 h <sup>-1</sup>	<ul style="list-style-type: none"> <li>• pH: 4.9 – 10</li> <li>• UV irradiation: 2.1 – 14.8 W m<sup>-2</sup></li> <li>• [NaOCl]: 0.03 – 0.63 mM</li> </ul>	[78]
	Simulated WW	1·10 <sup>-3</sup>	50 – 90%	-	<ul style="list-style-type: none"> <li>• pH: 7</li> <li>• UV: 40 – 200 W</li> <li>• [HOCl]: 0.008 – 0.116 mM</li> </ul>	[79]
	Simulated WW	1·10 <sup>-3</sup>	17 – 20%	-	<ul style="list-style-type: none"> <li>• pH: 7</li> <li>• UV: 40 – 200 W</li> <li>• [ClO<sub>2</sub>]: 0.003 – 0.092 mM</li> </ul>	[79]
UV/H <sub>2</sub> O <sub>2</sub>	Synthetic	2.5 – 10	63 – 100%	0.98 – 7.45 h <sup>-1</sup>	<ul style="list-style-type: none"> <li>• pH: 3 – 11</li> <li>• UV irradiation: 1.53 W m<sup>-2</sup></li> <li>• [H<sub>2</sub>O<sub>2</sub>]: 0.5 – 5 mM</li> </ul>	[44, 75]
	Synthetic and Spiked WWTP effluent	1	73 – 96%	-	<ul style="list-style-type: none"> <li>• [H<sub>2</sub>O<sub>2</sub>]: 0.5 mL L<sup>-1</sup></li> </ul>	[51]
	WWTP effluent	3.33·10 <sup>-4</sup>	82 – 99%	-	<ul style="list-style-type: none"> <li>• UV irradiation: 70 W m<sup>-2</sup></li> <li>• [H<sub>2</sub>O<sub>2</sub>]: 0.59 – 1.47 mM</li> </ul>	[3]
	WWTP effluent	0.043 ± 0.037	50 – 83%	-	<ul style="list-style-type: none"> <li>• Continuous operation</li> <li>• UV contact time: 9 – 28 s</li> <li>• pH: 7.17 ± 0.08</li> <li>• UV irradiation: 95.5 W m<sup>-2</sup></li> <li>• [H<sub>2</sub>O<sub>2</sub>]: 0.5 – 5 mM</li> </ul>	[76]
UV/O <sub>3</sub>	Synthetic and Spiked WWTP effluent	1	81 – 99%	-	<ul style="list-style-type: none"> <li>• O<sub>3</sub> flow: 2.6 g h<sup>-1</sup></li> <li>• UV lamp: 15 W</li> </ul>	[51]

	Spiked WWTP effluent	$1 \cdot 10^{-4}$	100%	-	<ul style="list-style-type: none"> <li>• Steady state time: 180 min</li> <li>• Hydraulic retention time: 41 min</li> <li>• pH: 8.5</li> <li>• <math>O_3</math>: <math>50 \text{ g Nm}^{-3}</math> (gas phase)</li> <li>• UV: 10 W (UVA-LEDs)</li> </ul>	[77]
UV/PMS	Synthetic	2.5 – 10	39 – 80%	$0.50 – 1.55 \text{ h}^{-1}$	<ul style="list-style-type: none"> <li>• pH: 3 – 11</li> <li>• UV irradiation: <math>1.53 \text{ W m}^{-2}</math></li> <li>• [PMS]: 0.5 – 5 mM</li> </ul>	[44, 75]
	WWTP effluent	$0.043 \pm 0.037$	73 – 100%	-	<ul style="list-style-type: none"> <li>• Continuous operation</li> <li>• UV contact time: 9 – 28 s</li> <li>• pH: <math>7.17 \pm 0.08</math></li> <li>• UV irradiation: <math>95.5 \text{ W m}^{-2}</math></li> <li>• [PMS]: 0.5 – 5 mM</li> </ul>	[76]
UV/PMS/Fe(II)	WWTP effluent	11.81	100%	$11.21 \pm 0.02 \text{ h}^{-1}$	<ul style="list-style-type: none"> <li>• pH: 3</li> <li>• Photonic flux: <math>7.9 \cdot 10^6 \text{ E min}^{-1}</math></li> <li>• [PMS]: 0.2 mM</li> <li>• [Fe(II)]: 0.1 mM</li> </ul>	[74]
	WWTP effluent	$0.043 \pm 0.037$	88 – 100%	-	<ul style="list-style-type: none"> <li>• Continuous operation</li> <li>• UV contact time: 9 – 28 s</li> <li>• pH: <math>7.17 \pm 0.08</math></li> <li>• UV irradiation: <math>95.5 \text{ W m}^{-2}</math></li> <li>• [PMS]: 0.5 – 5 mM</li> <li>• [Fe(II)]: 0.5 – 5 mM</li> </ul>	[76]
UV/PS	Synthetic	2.5 – 10	80 – 99%	$1.69 – 10.83 \text{ h}^{-1}$	<ul style="list-style-type: none"> <li>• pH: 3 – 11</li> <li>• UV irradiation: <math>1.53 \text{ W m}^{-2}</math></li> <li>• [PS]: 0.5 – 5 mM</li> </ul>	[44, 75]
	WWTP effluent	$0.043 \pm 0.037$	47 – 79%	-	<ul style="list-style-type: none"> <li>• Continuous operation</li> <li>• UV contact time: 9 – 28 s</li> <li>• pH: <math>7.17 \pm 0.08</math></li> <li>• UV irradiation: <math>95.5 \text{ W m}^{-2}</math></li> <li>• [PS]: 0.5 – 5 mM</li> </ul>	[76]
UV/PS/Fe(II)	WWTP effluent	$0.043 \pm 0.037$	96 – 100%	-	<ul style="list-style-type: none"> <li>• Continuous operation</li> <li>• UV contact time: 9 – 28 s</li> <li>• pH: <math>7.17 \pm 0.08</math></li> <li>• UV irradiation: <math>95.5 \text{ W m}^{-2}</math></li> <li>• [PS]: 0.5 – 5 mM</li> <li>• [Fe(II)]: 0.5 – 5 mM</li> </ul>	[76]

UV/TiO <sub>2</sub>	Synthetic	0.1	100%	10.44 h <sup>-1</sup>	<ul style="list-style-type: none"> <li>• Degussa P25 powders</li> <li>• Half-life time: 4.5 min</li> <li>• UV irradiation: 916 W m<sup>-2</sup></li> <li>• Energy: 3.30 kWh m<sup>-3</sup></li> </ul>	[80]
	Synthetic	0.1	65%	1.08 ± 0.42 h <sup>-1</sup>	<ul style="list-style-type: none"> <li>• TiO<sub>2</sub> mesh</li> <li>• Half-life time: 36 min</li> <li>• UV irradiation: 916 W m<sup>-2</sup></li> <li>• Energy: 31.98 kWh m<sup>-3</sup></li> </ul>	[80]
	Synthetic	1	60%	12.30 ± 0.66 h <sup>-1</sup>	<ul style="list-style-type: none"> <li>• Degussa P25</li> <li>• pH: 5</li> <li>• UV irradiance: 710 W m<sup>-2</sup></li> <li>• [P25]: 0.5 g L<sup>-1</sup></li> </ul>	[83]
	Spiked WWTP effluent	0.1	50 – 80%	-	<ul style="list-style-type: none"> <li>• TiO<sub>2</sub> immobilized on glass spheres</li> <li>• Natural sunlight</li> </ul>	[3]
	WWTP effluent	11.81	-	1.78 ± 0.01 h <sup>-1</sup>	<ul style="list-style-type: none"> <li>• pH: 7.8</li> <li>• Photonic flux: 7.9·10<sup>6</sup> E min<sup>-1</sup></li> <li>• [TiO<sub>2</sub>]: 0.5 g L<sup>-1</sup></li> </ul>	[74]
	WWTP effluent	2.95·10 <sup>-4</sup>	46 – 100%	0.92 h <sup>-1</sup>	<ul style="list-style-type: none"> <li>• TiO<sub>2</sub> nanoparticles</li> <li>• UV irradiance: 69 W m<sup>-2</sup></li> </ul>	[81]
	WWTP effluent	5 – 20	70 – 99%	1.02 – 4.50 h <sup>-1</sup>	<ul style="list-style-type: none"> <li>• Commercial TiO<sub>2</sub></li> <li>• pH: 3.4 – 10</li> <li>• UV irradiance: 15.08 ± 0.41 W m<sup>-2</sup></li> <li>• [TiO<sub>2</sub>]: 0.5 – 2 g L<sup>-1</sup></li> </ul>	[82]
Photo-Fenton	WWTP effluent	3.33·10 <sup>-4</sup>	66 – 94%	-	<ul style="list-style-type: none"> <li>• pH: 6 – 7.5</li> <li>• UV irradiation: 70 W m<sup>-2</sup></li> <li>• [H<sub>2</sub>O<sub>2</sub>]: 0.59 – 1.47 mM</li> <li>• [Fe]: 0.036 – 0.072 mM</li> </ul>	[3]
	WWTP effluent	0.1	100%	0.78 – 0.84 h <sup>-1</sup>	<ul style="list-style-type: none"> <li>• pH: 3</li> <li>• UV irradiation: 30 W m<sup>-2</sup></li> <li>• [H<sub>2</sub>O<sub>2</sub>]: 0.147 – 1.470 mM</li> <li>• [Fe]: 0.09 mM</li> </ul>	[56]
Other photocatalytic systems	Synthetic	1	99%	0.60 – 25.80 h <sup>-1</sup>	<ul style="list-style-type: none"> <li>• BiOCl<sub>0.875</sub>Br<sub>0.125</sub></li> <li>• pH: 4 – 9</li> <li>• UV irradiance: 710 W m<sup>-2</sup></li> <li>• [BiOCl<sub>0.875</sub>Br<sub>0.125</sub>]: 0.5 g L<sup>-1</sup></li> </ul>	[83]

Synthetic	5.91	80 – 100%	0.49 – 7.64 h <sup>-1</sup>	<ul style="list-style-type: none"> <li>• Triclinic-WO<sub>3</sub></li> <li>• pH: 4.6 – 6</li> <li>• UV lamp: 420 nm</li> <li>• UV intensity: 1.5·10<sup>-6</sup> E L<sup>-1</sup> s<sup>-1</sup></li> <li>• [WO<sub>3</sub>]: 0.3 g L<sup>-1</sup></li> <li>• [PS]: 2 mM</li> <li>• [CH<sub>3</sub>OH]: 0 – 100 mM</li> </ul>	[85]
Synthetic and Simulated WW	5	20 – 100%	0.12 – 7.86 h <sup>-1</sup>	<ul style="list-style-type: none"> <li>• BiPO<sub>4</sub> (hexagonal and monoclinic)</li> <li>• UV lamp: 100 W</li> <li>• [BiPO<sub>4</sub>]: 1 g L<sup>-1</sup></li> </ul>	[84]
WWTP effluent	2.95·10 <sup>-4</sup>	41 – 92%	0.84 h <sup>-1</sup>	<ul style="list-style-type: none"> <li>• ZnO nanoparticles</li> <li>• UV irradiance: 69 W m<sup>-2</sup></li> </ul>	[81]

**Table 2:** Summary of reported carbamazepine (CBZ) degradation in other methods for wastewater treatment.

Treatment	Matrix	Initial CBZ (mg L <sup>-1</sup> )	Removal	Rate constant	Comments	Ref.	
Advanced reduction processes	UV/Sulfite	Synthetic	5	5 – 99.6%	5.16 – 20.40 h <sup>-1</sup>	<ul style="list-style-type: none"> <li>pH: 3 – 11</li> <li>UV irradiation: 9 – 32 W m<sup>-2</sup></li> <li>[Sulfite]: 0 – 1.6 mM</li> </ul>	[40]
Biological treatment	Laccase	Synthetic	4.73	22 – 60%	-	<ul style="list-style-type: none"> <li>pH: 4.5</li> <li>[Laccase]: 10 nkat mL<sup>-1</sup></li> <li>[1-hydroxybenzotriazole]: 0 – 0.2 mM</li> <li>Culture: <i>T. versicolor</i></li> </ul>	[89]
	Lignin peroxidase	Synthetic	5	7 – 15%	-	<ul style="list-style-type: none"> <li>pH: 2.5 – 6</li> <li>[H<sub>2</sub>O<sub>2</sub>]: 0.7 mM</li> <li>Culture: <i>P. chrysosporium</i></li> </ul>	[90]
	Manganese peroxidase	Synthetic	4.73	14%	-	<ul style="list-style-type: none"> <li>pH: 4.5</li> <li>[MnP]: 10 nkat mL<sup>-1</sup></li> <li>[MnSO<sub>4</sub>]: 0.1 mM</li> <li>[Glucose]: 25 mM</li> <li>[Glucose oxidase]: 3.33 nkat mL<sup>-1</sup></li> <li>Culture: <i>P. chrysosporium</i></li> </ul>	[89]
	Multiple enzymes	Synthetic	10	47 – 58%	-	<ul style="list-style-type: none"> <li>Cultures: <i>T. versicolor</i>, <i>G. lucidum</i>, <i>I. lacteus</i>, <i>P. chrysosporium</i></li> </ul>	[93]
		Synthetic	1	99%	-	<ul style="list-style-type: none"> <li>Cultures: <i>Bjerkandera sp. R1</i>, <i>B. adusta</i>, <i>P. chrysosporium</i></li> </ul>	[91]
		Synthetic	1·10 <sup>-3</sup>	48 – 99%	-	<ul style="list-style-type: none"> <li>Cultures: <i>P. ostreatus Florida N001</i>, <i>P. ostreatus PC9</i>, <i>P. ostreatus Florida F6</i>.</li> </ul>	[87]
Enriched bacteria	WWTP effluent	10 – 40	10 – 46%	0.001 – 0.004 h <sup>-1</sup>	<ul style="list-style-type: none"> <li>Enriched sulfate-reducing and fermentative acidogenic bacteria compared to mixed microbial communities</li> <li>Influence of COD:SO<sub>4</sub><sup>2-</sup>- and CBZ dose</li> </ul>	[92]	
Physical treatment	PAC	WWTP effluent	2.21 – 4.62·10 <sup>-4</sup>	90 – 92%	-	<ul style="list-style-type: none"> <li>[PAC]: 10 – 20 mg m<sup>-1</sup></li> <li>20 – 60 min contact time</li> </ul>	[3]
	GAC	MWWTP effluent	1.10·10 <sup>-4</sup>	72%	-	<ul style="list-style-type: none"> <li>23,400 bed volumes treated</li> <li>14 min empty bed contact time</li> </ul>	[3]

MOFs	Synthetic	10	87 – 100%	$Q_m$ : 663.70 mg g <sup>-1</sup>	<ul style="list-style-type: none"> <li>• Comparison between MOF-5-derived nanoporous carbon, ZIF-8-derived nanoporous carbon and commercial PAC</li> </ul>	[99]
	Synthetic	1·10 <sup>-3</sup>	-	$K_F$ : 57.56 – 73.79 (ng/mg)(L/ng) <sup>1/n</sup>	<ul style="list-style-type: none"> <li>• Two GAC adsorbents</li> <li>• Carbon dosage: 10 – 800 ng L<sup>-1</sup></li> <li>• Adsorption equilibria after 12 days</li> <li>• (1/n) = 0.42 – 0.43</li> </ul>	[97]
NF	Groundwater	20	97 – 100%	-	<ul style="list-style-type: none"> <li>• pH: 5.6 – 6.1</li> <li>• Feed flow rate: 360 m<sup>3</sup> h<sup>-1</sup></li> <li>• Permeate flow rate: 234 m<sup>3</sup> h<sup>-1</sup></li> <li>• Filtration in two stages, comprising 31 and 15 membrane modules with 6 NF membranes each</li> </ul>	[105]
RO	Groundwater	20	99 – 100%	-	<ul style="list-style-type: none"> <li>• pH: 5.6 – 6.1</li> <li>• Feed flow rate: 486 m<sup>3</sup> h<sup>-1</sup></li> <li>• Permeate flow rate: 356.4 m<sup>3</sup> h<sup>-1</sup></li> <li>• Filtration in two stages, comprising 40 and 20 membrane modules with 6 RO membranes each</li> </ul>	[105]

## 612 **8 Conclusions**

613  
614 There is an urgent need to tackle the ubiquitous presence of recalcitrant contaminants in natural  
615 water bodies, which pose a potential threat to aquatic ecosystems and human health. As discussed  
616 in this review, advanced oxidation processes (AOPs) have been effective in the degradation of  
617 pharmaceutically active compounds such as carbamazepine, as opposed to biological and physical  
618 treatments. In particular, high degradation efficiencies have been attained through electrochemical  
619 and photocatalytic AOPs under multiple experimental conditions. However, future research should  
620 be dedicated to enhancing the adaptability and practicability of AOPs, such as by reducing chemical,  
621 energy and catalyst needs. In addition, their resilience against radical scavengers and wastewater  
622 components needs to be improved to promote their implementation at a larger scale. Finally, along  
623 with reporting degradation efficiencies of the targeted PhACs, studies should focus on elucidating  
624 the underlying degradation mechanisms to ensure that toxic byproducts are not discharged.  
625

## 626 **Acknowledgements**

627  
628  
629 The research leading to these results received funding from the European Union's EU Framework  
630 Programme for Research and Innovation Horizon 2020 under Grant Agreement No 861369 (MSCA-  
631 ETN InnovEOX) and from the KU Leuven Industrial Research Council under grant number  
632 C24E/19/040 (SO4ELECTRIC).  
633

## 634 **Competing interests**

635  
636  
637 The authors declare no competing interests.  
638

## 639 **References**

- 640  
641
- 642 [1] N. H. Tran, M. Reinhard, K. Y.-H. Gin, Occurrence and fate of emerging contaminants in  
643 municipal wastewater treatment plants from different geographical regions - A review, *Water*  
644 *Res.* 133 (2018) 182–207. doi:10.1016/j.watres.2017.12.029.
  - 645 [2] A. R. Ribeiro, O. C. Nunes, M. F. Pereira, A. M. Silva, An overview on the advanced oxidation  
646 processes applied for the treatment of water pollutants defined in the recently launched  
647 Directive 2013/39/EU, *Environ. Int.* 75 (2015) 33–51. doi:10.1016/j.envint.2014.10.027.
  - 648 [3] L. Rizzo, S. Malato, D. Antakyali, V. G. Beretsou, M. B. Dolic, W. Gernjak, E. Heath, I. Ivancev-  
649 Tumbas, P. Karaolia, A. R. Lado Ribeiro, G. Mascolo, C. S. McArdell, H. Schaar, A. M. T. Silva, D.  
650 Fatta-Kassinos, Consolidated vs new advanced treatment methods for the removal of  
651 contaminants of emerging concern from urban wastewater, *Sci. Total Environ.* 655 (2019)  
652 986–1008. doi:10.1016/j.scitotenv.2018.11.265.

- 653 [4] D. Seibert, C. F. Zorzo, F. H. Borba, R. M. de Souza, H. B. Quesada, R. Bergamasco, A. T. Baptista,  
654 J. J. Inticher, Occurrence, statutory guideline values and removal of contaminants of emerging  
655 concern by Electrochemical Advanced Oxidation Processes: A review, *Sci. Total Environ.* 748  
656 (2020) 141527. doi:10.1016/j.scitotenv.2020.141527.
- 657 [5] C. Teodosiu, A.-F. Gilca, G. Barjoveanu, S. Fiore, Emerging pollutants removal through advanced  
658 drinking water treatment: A review on processes and environmental performances assessment,  
659 *J. Clean. Prod.* 197 (2018) 1210–1221. doi:10.1016/j.jclepro.2018.06.247.
- 660 [6] E. M. Cuerda-Correa, M. F. Alexandre-Franco, C. Fernández-González, Advanced Oxidation  
661 Processes for the removal of antibiotics from water. An overview, *Water* 12 (1) (2020).  
662 doi:10.3390/w12010102.
- 663 [7] A. Boretti, L. Rosa, Reassessing the projections of the World Water Development Report, *npj*  
664 *Clean Water* 2 (2019). doi:10.1038/s41545-019-0039-9.
- 665 [8] D. E. Vidal-Dorsch, S. M. Bay, K. Maruya, S. A. Snyder, R. A. Trenholm, B. J. Vanderford,  
666 Contaminants of emerging concern in municipal wastewater effluents and marine receiving  
667 water, *Environ. Toxicol. Chem.* 31 (12) (2012) 2674–2682. doi:10.1002/etc.2004.
- 668 [9] J. M. Diamond, H. A. Latimer, K. R. Munkittrick, K. W. Thornton, S. M. Bartell, K. A. Kidd,  
669 Prioritizing contaminants of emerging concern for ecological screening assessments, *Environ.*  
670 *Toxicol. Chem.* 30 (11) (2011) 2385–2394.
- 671 [10] T. Nawaz, S. Sengupta, Chapter 4 - Contaminants of Emerging Concern: Occurrence, fate, and  
672 remediation (2018). doi:10.1016/B978-0-12-814790-0.00004-1.
- 673 [11] R. Benson, O. D. Conerly, W. Sander, A. L. Batt, J. S. Boone, E. T. Furlong, S. T. Glassmeyer, D. W.  
674 Kolpin, H. E. Mash, K. M. Schenck, J. E. Simmons, Human health screening and public health  
675 significance of contaminants of emerging concern detected in public water supplies, *Sci. Total*  
676 *Environ.* 579 (2017) 1643–1648. doi:10.1016/j.scitotenv.2016.03.146.
- 677 [12] E. Nilsen, K. L. Smalling, L. Ahrens, M. Gros, K. S. Miglioranza, Y. Picó, H. L. Schoenfuss, Critical  
678 review: Grand challenges in assessing the adverse effects of contaminants of emerging concern  
679 on aquatic food webs, *Environ. Toxicol. Chem.* 38 (2019) 46–60. doi:10.1002/etc.4290.
- 680 [13] G. Vandermeersch, H. M. Lourenço, D. Alvarez-Muñoz, S. Cunha, J. Diogène, G. Cano-Sancho, J.  
681 J. Sloth, C. Kwadijk, D. Barcelo, W. Allegaert, K. Bekaert, J. O. Fernandes, A. Marques, J.  
682 Robbens, Environmental contaminants of emerging concern in seafood – European database on  
683 contaminant levels, *Environ. Res.* 143 (2015) 29–45. doi:10.1016/j.envres.2015.06.011.
- 684 [14] O. Herrero, J. Pérez Martín, P. Fernández Freire, L. Carvajal López, A. Peropadre, M. Hazen,  
685 Toxicological evaluation of three contaminants of emerging concern by use of the *Allium cepa*  
686 test, *Mutat. Res. Genet. Toxicol. Environ. Mutagen.* 743 (1) (2012) 20–24.  
687 doi:10.1016/j.mrgentox.2011.12.028.
- 688 [15] K. A. Baken, R. M. Sjerps, M. Schriks, A. P. van Wezel, Toxicological risk assessment and  
689 prioritization of drinking water relevant contaminants of emerging concern, *Environ. Int.* 118  
690 (2018) 293–303. doi:10.1016/j.envint.2018.05.006.

- 691 [16] A. J. Balkema, H. A. Preisig, R. Otterpohl, F. J. Lambert, Indicators for the sustainability  
692 assessment of wastewater treatment systems, *Urban Water J.* 4 (2) (2002) 153–161.  
693 doi:10.1016/S1462-0758(02)00014-6.
- 694 [17] H. E. Muga, J. R. Mihelcic, Sustainability of wastewater treatment technologies, *J. Environ.*  
695 *Manage.* 88 (3) (2008) 437–447. doi:10.1016/j.jenvman.2007.03.008.
- 696 [18] L. Høibye, J. Clauson-Kaas, H. Wenzel, H. F. Larsen, B. N. Jacobsen, O. Dalgaard, Sustainability  
697 assessment of advanced wastewater treatment technologies, *Water Sci. Technol.* 58 (5) (2008)  
698 963–968. doi:10.2166/wst.2008.450.
- 699 [19] A. N. Bdour, M. R. Hamdi, Z. Tarawneh, Perspectives on sustainable wastewater treatment  
700 technologies and reuse options in the urban areas of the Mediterranean region, *Desalination*  
701 237 (1) (2009) 162–174. doi:10.1016/j.desal.2007.12.030.
- 702 [20] M. Molinos-Senante, T. Gómez, M. Garrido-Baserba, R. Caballero, R. Sala-Garrido, Assessing the  
703 sustainability of small wastewater treatment systems: A composite indicator approach, *Sci.*  
704 *Total Environ.* 497-498 (2014) 607–617. doi:10.1016/j.scitotenv.2014.08.026.
- 705 [21] H. Wu, J. Zhang, H. H. Ngo, W. Guo, Z. Hu, S. Liang, J. Fan, H. Liu, A review on the sustainability  
706 of constructed wetlands for wastewater treatment: Design and operation, *Bioresour. Technol.*  
707 175 (2015) 594–601. doi:10.1016/j.biortech.2014.10.068.
- 708 [22] A. G. Capodaglio, A. Callegari, D. Cecconet, D. Molognoni, Sustainability of decentralized  
709 wastewater treatment technologies, *Water Pract. Technol.* 12 (2) (2017) 463–477.  
710 doi:10.2166/wpt.2017.055.
- 711 [23] M. Kamali, K. M. Persson, M. E. Costa, I. Capela, Sustainability criteria for assessing  
712 nanotechnology applicability in industrial wastewater treatment: Current status and future  
713 outlook, *Environ. Int.* 125 (2019) 261–276. doi:10.1016/j.envint.2019.01.055.
- 714 [24] WebMD, Carbamazepine - Uses, Side Effects, and More, <https://www.webmd.com/drugs/2/drug-1493-5/carbamazepine-oral/carbamazepine-oral/details> (December 2021).  
715
- 716 [25] R. Oldenkamp, A. H. W. Beusen, M. A. J. Huijbregts, Aquatic risks from human  
717 pharmaceuticals—modelling temporal trends of carbamazepine and ciprofloxacin at the global  
718 scale, *Environ. Res. Lett.* 14 (3) (2019) 034003. doi:10.1088/1748-9326/ab0071.
- 719 [26] Y. Zhang, S.-U. Geißen, C. Gal, Carbamazepine and diclofenac: Removal in wastewater  
720 treatment plants and occurrence in water bodies, *Chemosphere* 73 (8) (2008) 1151–1161.  
721 doi:10.1016/j.chemosphere.2008.07.086.
- 722 [27] J. D. García-Espinoza, P. Miajaylova-Nacheva, M. Avilés-Flores, Electrochemical carbamazepine  
723 degradation: Effect of the generated active chlorine, transformation pathways and toxicity,  
724 *Chemosphere* 192 (2018) 142–151. doi:10.1016/j.chemosphere.2017.10.147.
- 725 [28] S. Ebrahimzadeh, S. Castiglioni, F. Riva, E. Zuccato, A. Azzellino, Carbamazepine levels related to  
726 the demographic indicators in groundwater of densely populated area, *Water* 13 (18) (2021).  
727 doi:10.3390/w13182539.

- 728 [29] J. L. Wilkinson, A. B. A. Boxall, D. W. Kolpin, K. M. Y. Leung, R. W. S. Lai, C. Galbán-Malagón, A. D.  
729 Adell, J. Mondon, M. Metian, R. A. Marchant, A. Bouzas-Monroy, A. Cuni-Sanchez, A. Coors, P.  
730 Carriquiriborde, M. Rojo, C. Gordon, M. Cara, M. Moermond, T. Luarte, V. Petrosyan, Y.  
731 Perikhanyan, C. S. Mahon, C. J. McGurk, T. Hofmann, T. Kormoker, V. Iniguez, J. Guzman-Otazo,  
732 J. L. Tavares, F. G. D. Figueiredo, M. T. P. Razzolini, V. Dougnon, G. Gbaguidi, O. Traoré, J. M.  
733 Blais, L. E. Kimpe, M. Wong, D. Wong, R. Ntchantcho, J. Pizarro, G.-G. Ying, C.-E. Chen, M. Páez,  
734 J. Martínez-Lara, J.-P. Otamonga, J. Poté, S. A. Ifo, P. Wilson, S. Echeverría-Sáenz, N. Udikovic-  
735 Kolic, M. Milakovic, D. Fatta-Kassinos, L. Ioannou-Ttofa, V. Belusová, J. Vymazal, M. Cárdenas-  
736 Bustamante, B. A. Kassa, J. Garric, A. Chaumot, P. Gibba, I. Kunchulia, S. Seidensticker, G.  
737 Lyberatos, H. P. Halldórsson, M. Melling, T. Shashidhar, M. Lamba, A. Nastiti, A. Supriatin, N.  
738 Pourang, A. Abedini, O. Abdullah, S. S. Gharbia, F. Pilla, B. Chefetz, T. Topaz, K. M. Yao, B.  
739 Aubakirova, R. Beisenova, L. Olaka, J. K. Mulu, P. Chatanga, V. Ntuli, N. T. Blama, S. Sherif, A. Z.  
740 Aris, L. J. Looi, M. Niang, S. T. Traore, R. Oldenkamp, O. Ogunbanwo, M. Ashfaq, M. Iqbal, Z.  
741 Abdeen, A. O’Dea, J. M. Morales-Saldaña, M. Custodio, H. de la Cruz, I. Navarrete, F. Carvalho,  
742 A. B. Gogra, B. M. Koroma, V. Cerkvenik-Flajs, M. Gombac, M. Thwala, K. Choi, H. Kang, J. L. C.  
743 Ladu, A. Rico, P. Amerasinghe, A. Sobek, G. Horlitz, A. K. Zenker, A. C. King, J.-J. Jiang, R. Kariuki,  
744 M. Tumbo, U. Tezel, T. T. Onay, J. B. Lejju, Y. Vystavna, Y. Vergeles, H. Heinzen, A. Pérez-Parada,  
745 D. B. Sims, M. Figy, D. Good, C. Teta, Pharmaceutical pollution of the world’s rivers, PNAS 119  
746 (8) (2022). doi:10.1073/pnas.2113947119.
- 747 [30] NORMAN-Network, NORMAN database system, <https://www.norman-network.com/nds/>  
748 (January 2021).
- 749 [31] N. Liu, Z.-D. Lei, T. Wang, J.-J. Wang, X.-D. Zhang, G. Xu, L. Tang, Radiolysis of carbamazepine  
750 aqueous solution using electron beam irradiation combining with hydrogen peroxide: Efficiency  
751 and mechanism, Chem. Eng. J. 295 (2016) 484–493.
- 752 [32] D. Mohapatra, S. Brar, R. Tyagi, P. Picard, R. Surampalli, Analysis and advanced oxidation  
753 treatment of a persistent pharmaceutical compound in wastewater and wastewater sludge-  
754 carbamazepine, Sci. Total Environ. 470-471 (2014) 58–75. doi:10.1016/j.scitotenv.2013.09.034.
- 755 [33] F. I. Hai, S. Yang, M. B. Asif, V. Sencadas, S. Shawkat, M. Sanderson-Smith, J. Gorman, Z.-Q. Xu,  
756 K. Yamamoto, Carbamazepine as a possible anthropogenic marker in water: Occurrences,  
757 toxicological effects, regulations and removal by wastewater treatment technologies, Water 10  
758 (2) (2018). doi:10.3390/w10020107.
- 759 [34] United States Environmental Protection Agency - USEPA, Endocrine Disruptor Screening  
760 Program. Universe of Chemicals (2012).
- 761 [35] T. Sangeetha, C. P. Rajneesh, W.-M. Yan, 15 - Integration of microbial electrolysis cells with  
762 anaerobic digestion to treat beer industry wastewater, in: R. Abbassi, A. K. Yadav,
- 763 [36] G. Crini, E. Lichtfouse, Advantages and disadvantages of techniques used for wastewater  
764 treatment, Environ. Chem. Lett. 17 (2019) 145–155. doi:10.1007/s10311-018-0785-9.
- 765 [37] Y. Deng, R. Zhao, Advanced Oxidation Processes (AOPs) in wastewater treatment, Water Pollut.  
766 1 (2015) 167–176. doi:10.1007/s40726-015-0015-z.

- 767 [38] U. Ushani, X. Lu, J. Wang, Z. Zhang, J. Dai, Y. Tan, S. Wang, W. Li, C. Niu, T. Cai, N. Wang, G. Zhen,  
768 Sulfate radicals-based advanced oxidation technology in various environmental remediation: A  
769 state-of-the-art review, *Chem. Eng. J.* 402 (2020). doi:10.1016/j.cej.2020.126232.
- 770 [39] X. Liu, S. Yoon, B. Batchelor, A. Abdel-Wahab, Photochemical degradation of vinyl chloride with  
771 an Advanced Reduction Process (ARP) - Effects of reagents and pH, *Chem. Eng. J.* 215-216  
772 (2013) 868–875. doi:10.1016/j.cej.2012.11.086.
- 773 [40] X. Yu, Z. Gocze, D. Cabooter, R. Dewil, Efficient reduction of carbamazepine using UV-activated  
774 sulfite: Assessment of critical process parameters and elucidation of radicals involved, *Chem.*  
775 *Eng. J.* 404 (2021). doi:10.1016/j.cej.2020.126403.
- 776 [41] B. P. Vellanki, B. Batchelor, A. Abdel-Wahab, Advanced Reduction Processes: A new class of  
777 treatment processes, *Environ. Eng. Sci.* 30 (5) (2013) 264–271. doi:10.1089/ees.2012.0273.
- 778 [42] A. R. Lado Ribeiro, N. F. Moreira, G. Li Puma, A. M. Silva, Impact of water matrix on the removal  
779 of micropollutants by advanced oxidation technologies, *Chem. Eng. J.* 363 (2019) 155–173.  
780 doi:10.1016/j.cej.2019.01.080.
- 781 [43] S. Garcia-Segura, J. D. Ocon, M. N. Chong, Electrochemical oxidation remediation of real  
782 wastewater effluents - A review, *Process Saf. Environ. Prot.* 113 (2018) 48–67.  
783 doi:10.1016/j.psep.2017.09.014.
- 784 [44] G. Boczka, A. Fernandes, Wastewater treatment by means of advanced oxidation processes at  
785 basic pH conditions: A review, *Chem. Eng. J.* 320 (2017) 608–633.  
786 doi:10.1016/j.cej.2017.03.084.
- 787 [45] I. F. Macías-Quiroga, P. A. Henao-Aguirre, A. Marín-Flórez, S. M. Arredondo-López, N. R.  
788 Sanabria-González, Bibliometric analysis of advanced oxidation processes (AOPs) in wastewater  
789 treatment: Global and Ibero-American research trends, *Environ. Sci. Pollut. Res.* (2020).  
790 doi:10.1007/s11356-020-11333-7.
- 791 [46] J. Garrido-Cardenas, B. Esteban-García, A. Agüera, J. Sánchez-Pérez, F. Manzano-Agugliaro,  
792 Wastewater treatment by Advanced Oxidation Process and their worldwide research trends,  
793 *Int. J. Environ. Res. Public Health* 17 (2020). doi:10.3390/ijerph17010170.
- 794 [47] J. Wang, R. Zhuan, Degradation of antibiotics by advanced oxidation processes: An overview,  
795 *Sci. Total Environ.* 701 (2020) 135023. doi:10.1016/j.scitotenv.2019.135023.
- 796 [48] S. Guerra-Rodríguez, E. Rodríguez, D. N. Singh, J. Rodríguez-Chueca, Assessment of Sulfate  
797 Radical-Based Advanced Oxidation Processes for water and wastewater treatment: A review,  
798 *Water* 10 (12) (2018). doi:10.3390/w10121828.
- 799 [49] S. Giannakis, K. Y. A. Lin, F. Ghanbari, A review of the recent advances on the treatment of  
800 industrial wastewaters by Sulfate Radical-based Advanced Oxidation Processes (SR- AOPs),  
801 *Chem. Eng. J.* 406 (2021) 127083. doi:10.1016/j.cej.2020.127083.
- 802 [50] D. C. McDowell, M. M. Huber, M. Wagner, U. Von Gunten, T. A. Ternes, Ozonation of  
803 carbamazepine in drinking water: Identification and kinetic study of major oxidation products,  
804 *Environ. Sci. Technol.* 39 (20) (2005) 8014–8022.

- 805 [51] W. Gebhardt, H. F. Schröder, Liquid chromatography–(tandem) mass spectrometry for the  
806 follow-up of the elimination of persistent pharmaceuticals during wastewater treatment  
807 applying biological wastewater treatment and advanced oxidation, *J. Chromatogr. A* 1160 (1)  
808 (2007) 34–43. doi:10.1016/j.chroma.2007.05.075.
- 809 [52] R. Juárez, S. Karlsson, P. Falas, °Asa Davidsson, K. Bester, M. Cimbritz, Integrating dissolved and  
810 particulate matter into a prediction tool for ozonation of organic micropollutants in  
811 wastewater, *Sci. Total Environ.* 795 (2021) 148711. doi:10.1016/j.scitotenv.2021.148711.
- 812 [53] E. Brillas, I. Sirés, M. A. Oturan, Electro-Fenton process and related electrochemical  
813 technologies based on Fenton’s reaction chemistry, *Chem. Rev.* 109 (12) (2009) 6570–6631.  
814 doi:10.1021/cr900136g.
- 815 [54] R. Matta, S. Tlili, S. Chiron, S. Barbati, Removal of carbamazepine from urban wastewater by  
816 sulfate radical oxidation, *Environ. Chem. Lett.* 9 (3) (2011) 347–353.
- 817 [55] W. Li, V. Nanaboina, Q. Zhou, G. V. Korshin, Effects of Fenton treatment on the properties of  
818 effluent organic matter and their relationships with the degradation of pharmaceuticals and  
819 personal care products, *Water Res.* 46 (2) (2012) 403–412. doi:10.1016/j.watres.2011.11.002.
- 820 [56] N. Klammerth, L. Rizzo, S. Malato, M. I. Maldonado, A. Agüera, A. Fernández-Alba, Degradation of  
821 fifteen emerging contaminants at  $\mu\text{g L}^{-1}$  initial concentrations by mild solar photo-Fenton in  
822 MWTP effluents, *Water Res.* 44 (2) (2010) 545–554. doi:10.1016/j.watres.2009.09.059.
- 823 [57] J. Wu, B. Wang, G. Cagnetta, J. Huang, Y. Wang, S. Deng, G. Yu, Nanoscale zero valent iron-  
824 activated persulfate coupled with Fenton oxidation process for typical pharmaceuticals and  
825 personal care products degradation, *Sep. Purif. Technol.* 239 (2020) 116534.  
826 doi:10.1016/j.seppur.2020.116534.
- 827 [58] B.-T. Zhang, Y. Zhang, Y. Teng, M. Fan, Sulfate radical and its application in decontamination  
828 technologies, *Crit. Rev. Env. Sci. Tec.* 45 (16) (2015) 1756–1800.  
829 doi:10.1080/10643389.2014.970681.
- 830 [59] Y. Rao, L. Qu, H. Yang, W. Chu, Degradation of carbamazepine by Fe(II)-activated persulfate  
831 process, *J. Hazard. Mater.* 268 (2014) 23–32. doi:10.1016/j.jhazmat.2014.01.010.
- 832 [60] J. Wu, G. Cagnetta, B. Wang, Y. Cui, S. Deng, Y. Wang, J. Huang, G. Yu, Efficient degradation of  
833 carbamazepine by organo-montmorillonite supported nCoFe<sub>2</sub>O<sub>4</sub>-activated peroxymonosulfate  
834 process, *Chem. Eng. J.* 368 (2019) 824–836. doi:10.1016/j.cej.2019.02.137.
- 835 [61] Q.-T. Sun, B.-D. Xu, J. Yang, T.-T. Qian, H. Jiang, Layered oxides supported Co-Fe bimetal catalyst  
836 for carbamazepine degradation via the catalytic activation of peroxymonosulfate, *Chem. Eng. J.*  
837 400 (2020) 125899. doi:10.1016/j.cej.2020.125899.
- 838 [62] S. Komtchou, A. Dirany, P. Drogui, A. Bermond, Removal of carbamazepine from spiked  
839 municipal wastewater using electro-Fenton process, *Environ. Sci. Pollut. Res.* 22 (15) (2015)  
840 11513–11525.

- 841 [63] C. García-Gómez, P. Drogui, F. Zavisca, B. Seyhi, P. Gortáres-Moroyoqui, G. Buelna, C. Neira-  
842 Sáenz, M. Estrada-alvarado, R. Ulloa-Mercado, Experimental design methodology applied to  
843 electrochemical oxidation of carbamazepine using Ti/PbO<sub>2</sub> and Ti/BDD electrodes, *J.*  
844 *Electroanal. Chem.* 732 (2014) 1–10. doi:10.1016/j.jelechem.2014.08.032.
- 845 [64] A. Farhat, J. Keller, S. Tait, J. Radjenovic, Removal of persistent organic contaminants by  
846 electrochemically activated sulfate, *Environ. Sci. Technol.* 49 (2015) 14326–14333.
- 847 [65] H. Song, L. Yan, J. Jiang, J. Ma, Z. Zhang, J. Zhang, P. Liu, T. Yang, Electrochemical activation of  
848 persulfates at BDD anode: Radical or nonradical oxidation?, *Water Res.* 128 (2018) 393–401.  
849 doi:10.1016/j.watres.2017.10.018.
- 850 [66] J. D. García-Espinoza, P. M. Nacheva, Degradation of pharmaceutical compounds in water by  
851 oxygenated electrochemical oxidation: Parametric optimization, kinetic studies and toxicity  
852 assessment, *Sci. Total Environ.* 691 (2019) 417–429. doi:10.1016/j.scitotenv.2019.07.118.
- 853 [67] J. D. García-Espinoza, P. Gortáres-Moroyoqui, M. T. Orta-Ledesma, P. Drogui, P. Mijaylova-  
854 Nacheva, Electrochemical removal of carbamazepine in water with Ti/PbO<sub>2</sub> cylindrical mesh  
855 anode, *Water Sci. Technol.* 73 (5) (2016) 1155–1165.
- 856 [68] N. Tran, P. Drogui, S. K. Brar, A. De Coninck, Synergistic effects of ultrasounds in the  
857 sonoelectrochemical oxidation of pharmaceutical carbamazepine pollutant, *Ultrason.*  
858 *Sonochem.* 34 (2017) 380–388. doi:10.1016/j.ultsonch.2016.06.014.
- 859 [69] K. Gurung, M. C. Ncibi, M. Shestakova, M. Sillanpää, Removal of carbamazepine from MBR  
860 effluent by electrochemical oxidation (EO) using a Ti/Ta<sub>2</sub>O<sub>5</sub>-SnO<sub>2</sub> electrode, *Appl. Catal. B* 221  
861 (2018) 329–338. doi:10.1016/j.apcatb.2017.09.017.
- 862 [70] L. Xu, J. Niu, H. Xie, X. Ma, Y. Zhu, J. Crittenden, Effective degradation of aqueous  
863 carbamazepine on a novel blue-colored TiO<sub>2</sub> nanotube arrays membrane filter anode, *J. Hazard.*  
864 *Mater.* 402 (2021) 123530.
- 865 [71] Y. Liu, B. Si, C. Zhao, F. Jin, H. Zheng, Z. Wang, Degradation of emerging contaminants by Co (III)  
866 ions in situ generated on anode surface in aqueous solution, *Chemosphere* 221 (2019) 543–553.  
867 doi:10.1016/j.chemosphere.2019.01.076.
- 868 [72] Y. Wang, F. A. Roddick, L. Fan, Direct and indirect photolysis of seven micropollutants in  
869 secondary effluent from a wastewater lagoon, *Chemosphere* 185 (2017) 297–308.  
870 doi:10.1016/j.chemosphere.2017.06.122.
- 871 [73] V. Calisto, M. R. M. Domingues, G. L. Erny, V. I. Esteves, Direct photodegradation of  
872 carbamazepine followed by micellar electrokinetic chromatography and mass spectrometry,  
873 *Water Res.* 45 (3) (2011) 1095–1104. doi:10.1016/j.watres.2010.10.037.
- 874 [74] M. M. Ahmed, M. Brienza, V. Goetz, S. Chiron, Solar photo-Fenton using peroxymonosulfate for  
875 organic micropollutants removal from domestic wastewater: Comparison with heterogeneous  
876 TiO<sub>2</sub> photocatalysis, *Chemosphere* 117 (2014) 256–261.  
877 doi:10.1016/j.chemosphere.2014.07.046.
- 878 [75] J. Deng, Y. Shao, N. Gao, S. Xia, C. Tan, S. Zhou, X. Hu, Degradation of the antiepileptic drug  
879 carbamazepine upon different UV-based advanced oxidation processes in water, *Chem. Eng. J.*  
880 222 (2013) 150–158. doi:10.1016/j.ccej.2013.02.045.

- 881 [76] J. Rodríguez-Chueca, C. García-Cañibano, M. Sarro, Ángel Encinas, C. Medana, D. Fabbri, P.  
882 Calza, J. Marugán, Evaluation of transformation products from chemical oxidation of  
883 micropollutants in wastewater by photoassisted generation of sulfate radicals, *Chemosphere*  
884 226 (2019) 509–519. doi:10.1016/j.chemosphere.2019.03.152.
- 885 [77] A. M. Gorito, J. F. Pesqueira, N. F. Moreira, A. R. Ribeiro, M. F. R. Pereira, O. C. Nunes, C. M. R.  
886 Almeida, A. M. Silva, Ozone-based water treatment (O<sub>3</sub>, O<sub>3</sub>/UV, O<sub>3</sub>/H<sub>2</sub>O<sub>2</sub>) for removal of organic  
887 micropollutants, bacteria inactivation and regrowth prevention, *J. Environ. Chem. Eng.* 9 (4)  
888 (2021) 105315. doi:10.1016/j.jece.2021.105315.
- 889 [78] W.-L. Wang, Q.-Y. Wu, N. Huang, T. Wang, H.-Y. Hu, Synergistic effect between UV and chlorine  
890 (UV/chlorine) on the degradation of carbamazepine: Influence factors and radical species,  
891 *Water Res.* 98 (2016) 190–198. doi:10.1016/j.watres.2016.04.015.
- 892 [79] C. Sichel, C. Garcia, K. Andre, Feasibility studies: UV/chlorine advanced oxidation treatment for  
893 the removal of emerging contaminants, *Water Res.* 45 (19) (2011) 6371–6380.  
894 doi:10.1016/j.watres.2011.09.025.
- 895 [80] S. Franz, E. Falletta, H. Arab, S. Murgolo, M. Bestetti, G. Mascolo, Degradation of carbamazepine  
896 by photo(electro)catalysis on nanostructured TiO<sub>2</sub> meshes: Transformation products and  
897 reaction pathways, *Catalysts* 10 (2) (2020). doi:10.3390/catal10020169.
- 898 [81] D. Mohapatra, S. Brar, R. Daghrir, R. Tyagi, P. Picard, R. Surampalli, P. Drogui, Photocatalytic  
899 degradation of carbamazepine in wastewater by using a new class of whey-stabilized  
900 nanocrystalline TiO<sub>2</sub> and ZnO, *Sci. Total Environ.* 485-486 (2014) 263–269.  
901 doi:10.1016/j.scitotenv.2014.03.089.
- 902 [82] A. Carabin, P. Drogui, D. Robert, Photo-degradation of carbamazepine using TiO<sub>2</sub> suspended  
903 photocatalysts, *J. Taiwan Inst. Chem. Eng.* 54 (2015) 109–117. doi:10.1016/j.jtice.2015.03.006.
- 904 [83] Y. Lester, D. Avisar, H. Gnayem, Y. Sasson, M. Shavit, H. Mamane, Demonstrating a new  
905 BiOCl<sub>0.875</sub>Br<sub>0.125</sub> photocatalyst to degrade pharmaceuticals under solar irradiation, *Water Air Soil*  
906 *Pollut.* 225 (9) (2014) 1–11.
- 907 [84] J. Xu, L. Li, C. Guo, Y. Zhang, W. Meng, Photocatalytic degradation of carbamazepine by tailored  
908 BiPO<sub>4</sub>: Efficiency, intermediates and pathway, *Appl. Catal. B* 130-131 (2013) 285–292.  
909 doi:10.1016/j.apcatb.2012.11.013.
- 910 [85] Y. Rao, W. Chu, Y. Wang, Photocatalytic oxidation of carbamazepine in triclinic-WO<sub>3</sub> suspension:  
911 Role of alcohol and sulfate radicals in the degradation pathway, *Appl. Catal. A-Gen* 468 (2013)  
912 240–249. doi:10.1016/j.apcata.2013.08.050.
- 913 [86] J. Cui, P. Gao, Y. Deng, Destruction of per- and polyfluoroalkyl substances (PFAS) with Advanced  
914 Reduction Processes (ARPs): A critical review, *Environ. Sci. Technol.* 54 (7) (2020) 3752–3766.  
915 doi:10.1021/acs.est.9b05565.
- 916 [87] K. Tahir, W. Miran, J. Jang, A. Shahzad, M. Moztahida, B. Kim, S.-R. Lim, D. S. Lee,  
917 Carbamazepine biodegradation and volatile fatty acids production by selectively enriched  
918 sulfate-reducing bacteria and fermentative acidogenic bacteria, *J. Chem. Technol. Biotechnol.*  
919 96 (3) (2021) 592–602. doi:10.1002/jctb.6572.
- 920 [88] S. Wang, J. Wang, Carbamazepine degradation by gamma irradiation coupled to biological  
921 treatment, *J. Hazard. Mater.* 321 (2017) 639–646. doi:10.1016/j.jhazmat.2016.09.053.

- 922 [89] T. Hata, H. Shintate, S. Kawai, H. Okamura, T. Nishida, Elimination of carbamazepine by  
923 repeated treatment with laccase in the presence of 1-hydroxybenzotriazole, *J. Hazard. Mater.*  
924 181 (1) (2010) 1175–1178. doi:10.1016/j.jhazmat.2010.05.103.
- 925 [90] Y. Zhang, S.-U. Geißén, In vitro degradation of carbamazepine and diclofenac by crude lignin  
926 peroxidase, *J. Hazard. Mater.* 176 (1) (2010) 1089–1092. doi:10.1016/j.jhazmat.2009.10.133.
- 927 [91] A. Rodarte-Morales, G. Feijoo, M. Moreira, J. Lema, Degradation of selected pharmaceutical and  
928 personal care products (PPCPs) by white-rot fungi, *World J. Microbiol. Biotechnol.* 27 (8) (2011)  
929 1839–1846. doi:10.1007/s11274-010-0642-x.
- 930 [92] N. Golan-Rozen, B. Chefetz, J. Ben-Ari, J. Geva, Y. Hadar, Transformation of the recalcitrant  
931 pharmaceutical compound carbamazepine by *pleurotus ostreatus*: Role of cytochrome P450  
932 monooxygenase and manganese peroxidase, *Environ. Sci. Technol.* 45 (16) (2011) 6800–6805.  
933 doi:10.1021/es200298t.
- 934 [93] E. Marco-Urrea, M. Pérez-Trujillo, T. Vicent, G. Caminal, Ability of white-rot fungi to remove  
935 selected pharmaceuticals and identification of degradation products of ibuprofen by *Trametes*  
936 *versicolor*, *Chemosphere* 74 (6) (2009) 765–772. doi:10.1016/j.chemosphere.2008.10.040.
- 937 [94] R. Guillosoy, J. Le Roux, R. Mailler, E. Vulliet, C. Morlay, F. Nauleau, J. Gasperi, V. Rocher,  
938 Organic micropollutants in a large wastewater treatment plant: What are the benefits of an  
939 advanced treatment by activated carbon adsorption in comparison to conventional treatment?,  
940 *Chemosphere* 218 (2019) 1050–1060. doi:10.1016/j.chemosphere.2018.11.182.
- 941 [95] F. Benstoem, A. Nahrstedt, M. Boehler, G. Knopp, D. Montag, H. Siegrist, J. Pinnekamp,  
942 Performance of granular activated carbon to remove micropollutants from municipal  
943 wastewater - A meta-analysis of pilot- and large-scale studies, *Chemosphere* 185 (2017) 105–  
944 118. doi:10.1016/j.chemosphere.2017.06.118.
- 945 [96] M. Boehler, B. Zwickelpflug, J. Hollender, T. Ternes, A. Joss, H. Siegrist, Removal of  
946 micropollutants in municipal wastewater treatment plants by powder-activated carbon, *Water*  
947 *Sci. Technol.* 66 (10) (2012) 2115–2121. doi:10.2166/wst.2012.353.
- 948 [97] Z. Yu, S. Peldszus, P. M. Huck, Adsorption characteristics of selected pharmaceuticals and an  
949 endocrine disrupting compound – naproxen, carbamazepine and nonylphenol – on activated  
950 carbon, *Water Res.* 42 (12) (2008) 2873–2882. doi:10.1016/j.watres.2008.02.020.
- 951 [98] S. Joseph, G. Saianand, M. R. Benzigar, K. Ramadass, G. Singh, A.-I. Gopalan, J. H. Yang, T. Mori,  
952 A. H. Al-Muhtaseb, J. Yi, A. Vinu, Recent advances in functionalized nanoporous carbons derived  
953 from waste resources and their applications in energy and environment, *Adv. Sustain. Syst.* 5 (1)  
954 (2021) 2000169. doi:10.1002/adsu.202000169.
- 955 [99] Y. Yu, D. Chen, S. Xie, Q. Sun, Z.-X. Zhang, G. Zeng, Adsorption behavior of carbamazepine on Zn-  
956 MOFs derived nanoporous carbons: Defect enhancement, role of N doping and adsorption  
957 mechanism, *J. Environ. Chem. Eng.* 10 (3) (2022) 107660. doi:10.1016/j.jece.2022.107660.

- 958 [100] M.-H. To, P. Hadi, C.-W. Hui, C. S. K. Lin, G. McKay, Mechanistic study of atenolol, acebutolol  
959 and carbamazepine adsorption on waste biomass derived activated carbon, *J. Mol. Liq.* 241  
960 (2017) 386–398. doi:10.1016/j.molliq.2017.05.037.
- 961 [101] D. Chen, H. Sun, Y. Wang, H. Quan, Z. Ruan, Z. Ren, X. Luo, UiO-66 derived zirconia/porous  
962 carbon nanocomposites for efficient removal of carbamazepine and adsorption mechanism,  
963 *Appl. Surf. Sci.* 507 (2020) 145054. doi:10.1016/j.apsusc.2019.145054.
- 964 [102] D. Chen, S. Wang, Z. Zhang, H. Quan, Y. Wang, Y. Jiang, M. J. Hurlock, Q. Zhang, Molten NaCl-  
965 induced MOF-derived carbon-polyhedron decorated carbon-nanosheet with high defects and  
966 high N-doping for boosting the removal of carbamazepine from water, *Environ. Sci. Nano* 7  
967 (2020) 1205–1213. doi:10.1039/C9EN01408J.
- 968 [103] D. Chen, S. Xie, C. Chen, H. Quan, L. Hua, X. Luo, L. Guo, Activated biochar derived from pomelo  
969 peel as a high-capacity sorbent for removal of carbamazepine from aqueous solution, *RSC Adv.*  
970 7 (2017) 54969–54979. doi:10.1039/C7RA10805B.
- 971 [104] M. Baghdadi, E. Ghaffari, B. Aminzadeh, Removal of carbamazepine from municipal wastewater  
972 effluent using optimally synthesized magnetic activated carbon: Adsorption and sedimentation  
973 kinetic studies, *J. Environ. Chem. Eng.* 4 (3) (2016) 3309–3321. doi:10.1016/j.jece.2016.06.034.
- 974 [105] J. Radjenovic, M. Petrovic, F. Ventura, D. Barceló, Rejection of pharmaceuticals in nanofiltration  
975 and reverse osmosis membrane drinking water treatment, *Water Res.* 42 (14) (2008) 3601–  
976 3610. doi:10.1016/j.watres.2008.05.020.
- 977 [106] A. Ghauch, H. Baydoun, P. Dermesropian, Degradation of aqueous carbamazepine in  
978 ultrasonic/Fe<sup>0</sup>/H<sub>2</sub>O<sub>2</sub> systems, *Chem. Eng. J.* 172 (1) (2011) 18–27. doi:10.1016/j.cej.2011.04.002.
- 979 [107] R. Dagherir, P. Drogui, A. Dimboukou-Mpira, M. El Khakani, Photoelectrocatalytic degradation of  
980 carbamazepine using Ti/TiO<sub>2</sub> nanostructured electrodes deposited by means of a pulsed laser  
981 deposition process, *Chemosphere* 93 (11) (2013) 2756–2766.  
982 doi:10.1016/j.chemosphere.2013.09.031.
- 983 [108] J. Monteagudo, A. Durán, R. González, A. Expósito, In situ chemical oxidation of carbamazepine  
984 solutions using persulfate simultaneously activated by heat energy, UV light, Fe<sup>2+</sup> ions, and  
985 H<sub>2</sub>O<sub>2</sub>, *Appl. Catal. B* 176-177 (2015) 120–129. doi:10.1016/j.apcatb.2015.03.055.